

Air Toxics Hot Spots Program

Perchloroethylene Inhalation Cancer Unit Risk Factor

Technical Support Document for Cancer
Potency Factors

Appendix B

SRP Review Draft

May 2016 (revised)



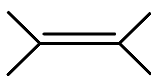
Air, Community, and Environmental Research Branch
Office of Environmental Health Hazard Assessment
California Environmental Protection Agency

Page left intentionally blank

List of Acronyms

AIC	Akaike information criterion	MCL	Mononuclear cell leukemia
AUC	Area under the concentration curve	MCMC	Markov Chain Monte Carlo method
BMD	Benchmark Dose	mg-hr/(L-d)	Milligram-hours per liter per day
BMDL	Estimation of the BMD 95% lower	mg/kg-d	Milligram per kilogram per day
BMDs	Benchmark Dose Software	µg/m ³	Microgram per cubic meter
BW	Body weight	MLE	Maximum likelihood estimate
CDPH	California Department of Health Services	MOA	Mode of action
CYP450	Cytochrome P450	N-AcTCVC	N-acetyl-S-(1,2,2-trichlorovinyl)cysteine
DCA	Dichloroacetic acid	NAT	N-acetyl transferase
DEHP	Diethyl hexyl phthalate	NCI	National Cancer Institute
DNA	Deoxyribose nucleic acid	NRC	National Research Council
DCVG	S-(1,2-dichlorovinyl)-glutathione	NTP	National Toxicology Program
FMO3	Flavin-containing mono-oxygenase 3	PBPK	Physiologically-based pharmacokinetic
GLP	Good Laboratory Practice standards	PCE	Perchloroethylene
GSH	Glutathione	PHG	Public Health Goal
GST	Glutathione-S-transferase	PPARα	Peroxisome proliferator-activated receptor-α
HEC	Human equivalent concentration	ppb	Parts per billion
IARC	International Agency for Research on Cancer	ppm	Parts per million
IRIS	Integrated risk information system (US EPA)	TAC	Toxic Air Contaminant
JBRC	Japan Bioassay Research Center	TCA	Trichloroacetic acid
JISHA	Japan Industrial Safety and Health Association	TCE	Trichloroethylene
LGLL	Large granular lymphocyte leukemia	TCVC	S-(trichlorovinyl)cysteine
		TCVG	S-(1,2,2-trichlorovinyl)-glutathione
		TSD	Technical Support Document
		URF	Unit risk factor
		US EPA	U.S. Environmental Protection Agency
		VOC	Volatile organic compound

1
2
PERCHLOROETHYLENE



3
4
5
6
CAS Number: 127-18-4

7
8
9
10
11
12
13
1. INTRODUCTION

14
15
16
17
18
19
20
21
22
23
The Office of Environmental Health Hazard Assessment (OEHHA) develops potency values for carcinogenic substances that are candidate Toxic Air Contaminants (TACs) (Health and Safety Code Section 39660) or are listed under the Air Toxics Hot Spots Act (Health and Safety Code Section 44321). These values are used in the Air Resources Board's (ARB's) air toxics control programs and also by other State regulatory bodies, to estimate cancer risk in humans.

14
15
16
17
18
19
20
21
22
23
Perchloroethylene (PCE), also commonly referred to as tetrachloroethylene, was officially placed on the TAC list by the ARB in 1991. In support of that decision, the California Department of Health Services evaluated the toxicology of PCE and determined that it was a potential carcinogen in humans, besides displaying other forms of toxicity (CDHS, 1991). Shortly thereafter, OEHHA derived inhalation potency values for PCE using dose-response data from a National Toxicology Program (NTP) study of the chemical's carcinogenic effects in rodents (OEHHA, 1992; NTP, 1986). OEHHA's potency values were based upon the induction of liver tumors in male mice and incorporated a simple pharmacokinetic model to estimate internal metabolized doses.

24
25
26
27
28
29
30
31
32
33
34
35
36
37
The present document updates the dose-response analysis for inhalation exposure to PCE to derive a cancer unit risk factor (expressed as $(\mu\text{g}/\text{m}^3)^{-1}$) and a corresponding cancer slope factor (expressed in $(\text{mg}/\text{kg}\cdot\text{d})^{-1}$) using OEHHA's current Air Toxics Hot Spots program risk assessment guidelines (OEHHA, 2009), and research made available since our last PCE review in 1992. In particular, OEHHA has identified an additional well-conducted, lifetime rodent inhalation study (JISHA, 1993); also, a refined physiologically-based pharmacokinetic (PBPK) model for PCE has been published (Chiu and Ginsberg, 2011). Both of these studies were used in the update. Where appropriate, the current analysis draws upon material from previous OEHHA evaluations, as well as recent toxicological assessments published by the US Environmental Protection Agency (US EPA, 2012a) and the International Agency for Research on Cancer (IARC, 2014).

38
39
40
41
42
2. SUMMARY OF DERIVED VALUES

38
39
40
41
42
OEHHA's revised potency values for PCE are based on the elevated incidence of several tumor types observed in male mice and rats in relation to PCE-metabolized doses calculated with a simplified adaptation of the Chiu and Ginsberg (2011) model. For dose-response calculations, OEHHA used US EPA's Benchmark Dose Software (BMDS) (US EPA, 2015) and its implementation of the multi-stage cancer model. BMDS was also

1 used to evaluate the multi-site tumor risks. After considering several issues related to
2 data quality and analytical uncertainty, the geometric mean of 4 dose-response values
3 was chosen as the best estimate of carcinogenic potency. The potency values for PCE,
4 in terms of external exposure, are:
5

Unit Risk Factor ($\mu\text{g}/\text{m}^3$) ⁻¹	6.1E-06
Slope Factor ($\text{mg}/\text{kg}\cdot\text{day}$) ⁻¹	2.1E-02

6 7 **3. MAJOR SOURCES AND USES**

8 PCE is a dense volatile liquid with an ether-like odor. It is used mainly as a chemical
9 intermediate, solvent, and cleaning agent. The total US demand for PCE in 2004 was
10 355 million pounds (Dow, 2008). In the US, 60 percent of PCE use was for chemical
11 production (e.g., to make hydrofluorocarbon alternatives to chlorofluorocarbons), 18
12 percent was used in surface preparation and cleaning, 18 percent in dry-cleaning and
13 textile processing, and 4 percent for miscellaneous other uses (*ibid.*). Total air
14 emissions of PCE in California for 2010 were estimated by ARB to be 3832 tons per
15 year (ARB, 2012).
16

17 **4. SELECTED PHYSICAL AND CHEMICAL PROPERTIES OF PCE**

18

Molecular weight	165.83
Boiling point	121 °C
Melting point	-19 °C
Vapor pressure	18.47 mm Hg @ 25 °C
Air concentration conversion	1 ppm = 6.78 mg/m ³ @ 25 °C

(HSDB, 2010)

19 20 **5. NATIONAL AND INTERNATIONAL HAZARD EVALUATIONS**

21 According to the National Toxicology Program (NTP) 13th Report on Carcinogens
22 (RoC), PCE is "reasonably anticipated to be a human carcinogen based on sufficient
23 evidence of carcinogenicity from studies in experimental animals" (NTP, 2014). The
24 RoC found that PCE exposure produced tumors in multiple tissue types of both sexes of
25 mice and rats. For inhalation exposure, the tumor types cited by NTP were:
26 mononuclear-cell leukemia in rats, tubular-cell kidney tumors in male rats and liver
27 tumors in mice. Additionally, NTP noted increased liver tumors in mice exposed to PCE
28 by ingestion.
29

30 IARC found that PCE is "probably carcinogenic to humans," citing limited
31 epidemiological findings (primarily increased bladder cancer in dry cleaning workers)
32 and sufficient evidence in experimental animals (IARC, 2014). For rodents, in addition to
33 the tumor types noted by NTP, IARC notes an increased incidence of: hemangioma and
34 hemangiosarcoma of the liver in mice, spleen and Harderian gland tumors in male mice,

1 brain and testicular tumors in male rats, and skin tumors in mice dermally exposed to
2 the PCE metabolite, tetrachloroethylene oxide.

3
4 US EPA states that PCE is “likely to be carcinogenic in humans by all routes of
5 exposure,” based upon suggestive epidemiologic data (bladder cancer, non-Hodgkin’s
6 lymphoma, and multiple myeloma) and conclusive evidence from carcinogenicity
7 studies in rodents (referring to the same set of tumors as above) (US EPA, 2012b).

8
9 PCE has been listed on California’s Proposition 65 list since 1988 as a chemical “known
10 to the state to cause cancer.” California’s Public Health Goal for drinking water is based
11 on PCE-induced carcinogenicity (OEHHA, 2001).

12 13 **6. TOXICOKINETICS**

14 PCE is readily absorbed through the lungs and gastrointestinal tract, and can also be
15 absorbed to a lesser extent through the skin. The blood-air partition coefficients of PCE
16 in humans and rodents are in the range of about 15 to 20 (Chiu and Ginsberg, 2011).
17 These values indicate the ratio by which the PCE concentration in blood will be greater
18 than its concentration in air at equilibrium. Humans breathing air containing 100 ppm
19 PCE over 8 hours absorbed approximately 70 percent of inhaled PCE after the first
20 hour, and 50 percent of the PCE intake at the end of the exposure period (Fernandez,
21 *et al.*, 1976). Once in the body, PCE disperses into all tissues, concentrating
22 preferentially in fatty tissues. For example, in rats inhaling 500 ppm PCE for 2 hours, the
23 area under the concentration curve (AUC) after 72 hours, in milligram-minutes per
24 milliliter of tissue, was: 1493 (fat), 33 (brain), 31 (liver), 26 (kidney), and 8.4 (blood)
25 (Dallas, *et al.*, 1994).

26
27 PCE has a relatively low rate of metabolism in rodents and humans and is primarily
28 eliminated unchanged via exhalation. In rats exposed to 150 ppm PCE in drinking water
29 for 12 hours and monitored for an additional 72 hours, approximately 88% of the body
30 burden was eliminated unmetabolized by exhalation (Frantz and Watanabe, 1983).
31 Ohtsuki, *et al.* (1983) monitored occupationally exposed dry-cleaning workers and
32 estimated that at the end of an 8-hour exposure to 50 ppm, about 38% of absorbed
33 PCE was exhaled unchanged and 2% metabolized and excreted in urine.

34 35 PCE Metabolites

36 The metabolism of perchloroethylene has been studied mostly in mice, rats, and
37 humans. Detailed reviews of this literature have been published (Lash and Parker,
38 2001; Anders *et al.*, 1988; Dekant, 1986). Briefly, rodent studies have identified the
39 following urinary metabolites:

- 40
41
- 42 • trichloroacetic acid (TCA)
 - 43 • N-trichloroacetyl aminoethanol
 - 44 • oxalic acid
 - 45 • N-oxalylaminoethanol
 - dichloroacetic acid (DCA)

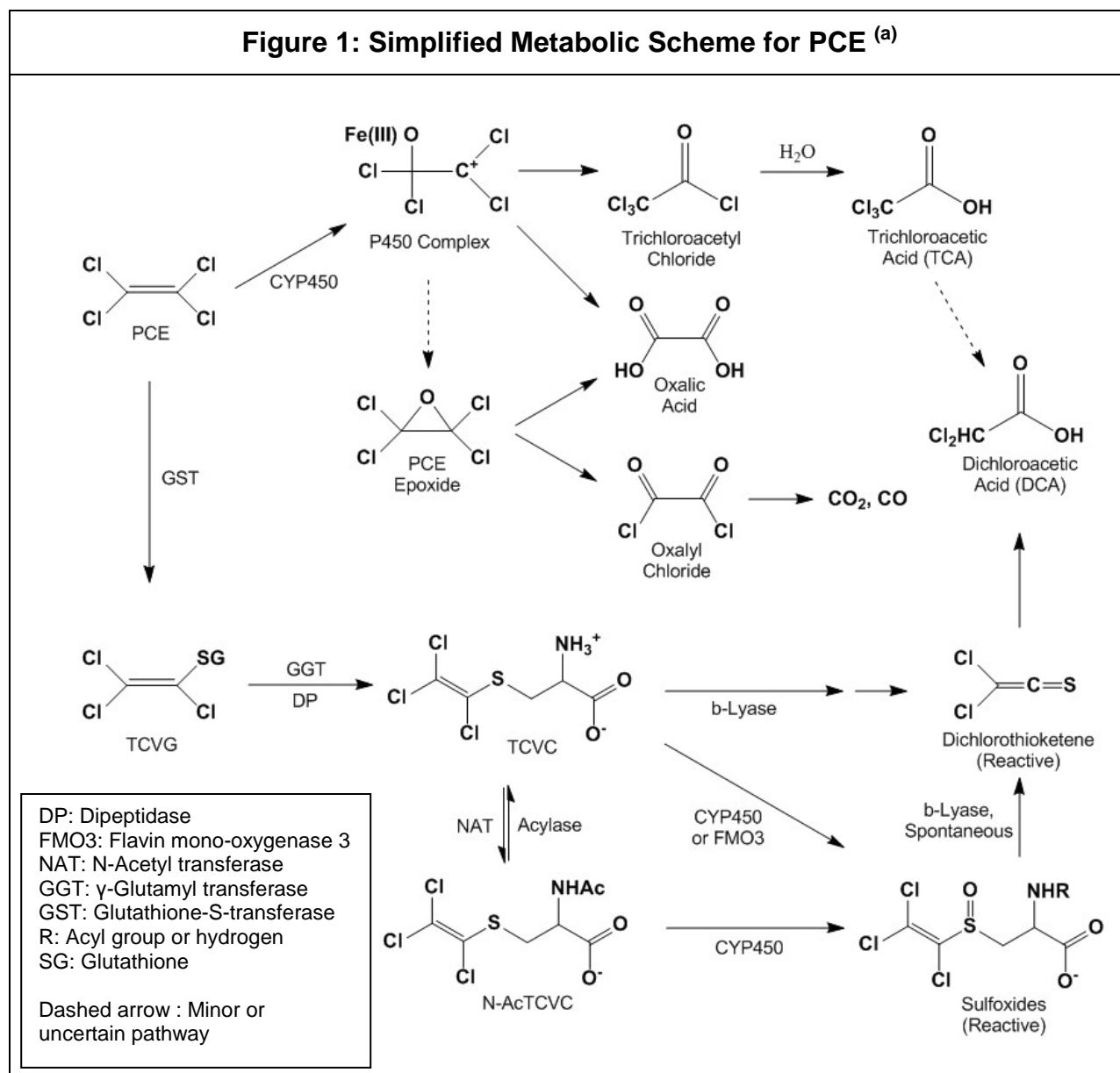
- 1 • S-(1,2,2-trichlorovinyl)glutathione (TCVG)
- 2 • N-acetyl-S-(1,2,2-trichlorovinyl)cysteine (N-AcTCVC)

3
4 Trichloroacetic acid and N-AcTCVC have also been observed in the urine of exposed
5 humans. The aminoethanol derivatives, N-trichloroacetyl aminoethanol and oxalyl
6 aminoethanol, are thought to arise from the reaction of the intermediate acyl chlorides
7 with phosphatidyl ethanolamine present in biological membranes (Dekant, *et al.*, 1986).
8 Carbon dioxide has also been found as an exhaled metabolite. Trichloroethanol has
9 been detected in urine samples in some studies, but not in others, and it is unclear
10 whether it was produced from co-exposure to trichloroethylene (in occupational
11 exposures), or in other cases, if it was an artifact of the analytical methods employed
12 (Lash and Parker, 2001). More recent work (e.g., Yoshioka, *et al.*, 2002) has not
13 detected trichloroethanol and supports the conclusion that it is not a significant PCE
14 metabolite (US EPA, 2012a).

15
16 A simplified metabolic scheme for PCE is presented in Figure 1. Two main pathways of
17 metabolism have been identified. The first, referred to here as the "oxidative pathway,"
18 involves oxidation of PCE by Cytochrome P450 (CYP450) enzymes. CYP2E1 is thought
19 to be the primary isoform involved, with additional participation of isoforms 2B1/2, and
20 3A4. The main metabolic product of the oxidative pathway is trichloroacetic acid (TCA),
21 formed by hydrolysis of intermediate trichloroacetyl chloride, the latter of which appears
22 to be formed by molecular rearrangement of the substrate-CYP450 complex (Guyton, *et al.*,
23 2014). A secondary product is the reactive tetrachloroethylene oxide (PCE epoxide),
24 which decomposes to oxalyl chloride and then to carbon monoxide and carbon dioxide
25 (Yoshioka, *et al.*, 2002). Oxalic acid may also form from decomposition of PCE epoxide
26 or directly from the substrate-enzyme complex. (Guyton *et al.*, 2014).

27
28 The second metabolic pathway for PCE (the "GST pathway") is initiated by glutathione-
29 S-transferase (GST)-catalyzed conjugation with glutathione (GSH), forming S-
30 (trichlorovinyl)glutathione (TCVG). This conjugate can undergo additional enzymatic
31 transformations to reactive and potentially genotoxic intermediates. First, the tripeptide
32 glutathione moiety of TCVG is degraded via hydrolytic cleavage of its glycine and
33 glutamine units, producing S-(trichlorovinyl)cysteine (TCVC). TCVC may be
34 subsequently transformed as follows:

- 35
36 • The free amino group of TCVC may be acylated by N-acetyl transferase, forming
37 N-acetyl-S-(trichlorovinyl)cysteine (N-AcTCVC) which passes into urine; this
38 process may also be reversed by acylases, regenerating TCVC.
- 39 • The sulfur atom of TCVC and N-AcTCVC may be oxidized by CYP450 or flavin-
40 containing mono-oxygenase 3 (FMO3); this process forms reactive α,β -
41 unsaturated sulfoxides that can bond with nucleophilic biological molecules or
42 spontaneously decompose to dichlorothioketene, itself a reactive metabolite.



(a) From Guyton *et al.* (2014), US EPA (2012a), and Lash and Parker (2001).

- 1 • The carbon-sulfur bond of TCVC may be cleaved by β -lyase, releasing an
- 2 unstable trichlorovinyl thiol that spontaneously decomposes to
- 3 dichlorothioketene.
- 4
- 5 Dichloroacetic acid, believed to arise mainly by hydrolysis of dichlorothioketene, was
- 6 found in rat but not human urine. Evidence for this mechanism comes from the detection
- 7 of a covalent protein adduct N-(dichloroacetyl)-L-lysine in rat kidney cells (Birner *et al.*,
- 8 1994).

1 Multi-Organ Metabolism

2 The toxicokinetic behavior of PCE is somewhat complicated due to the variety of
3 potentially genotoxic metabolites that can be produced, and because significant PCE
4 metabolism occurs in both the liver and kidney (and possibly other organs as well). The
5 liver is considered the main site of metabolism for the oxidative pathway. In this pathway,
6 initial oxidation by CYP450, produces several reactive intermediates that can rearrange,
7 hydrolyze, undergo conjugation, and otherwise decompose to more stable and soluble
8 metabolites that can then be eliminated in the urine or by exhalation. Other tissues with
9 appropriate CYP450 activity, e.g., lung, kidney, brain, and lymphocytes,¹ may also
10 independently oxidize PCE, though to a smaller extent.

11
12 The GST pathway involves a series of enzymatic transformations with cycling of
13 metabolic intermediates mainly between the liver and kidney, and including some entero-
14 hepatic processing. In this pathway, the initial glutathione conjugation step occurs
15 primarily in the liver, forming TCVG which is then transported to the blood and bile. The
16 kidney epithelium actively absorbs the circulating glutathione conjugate for further
17 processing and excretion. As noted above, this involves cleavage of TCVG by gamma
18 glutamyl transferase (GGT) and dipeptidase (DP) to form TCVC. The amino group of
19 TCVC can then be acylated to form mercapturate N-AcTCVC in the kidney, or TCVC
20 may recirculate back to the liver for acylation (Lash and Parker, 2001).

21
22 In some species, such as rabbit and guinea pig, significant intrahepatic processing of
23 glutathione conjugates may occur, with formation of TCVC from TCVG by the bile-duct
24 epithelium, followed by reabsorption into hepatocytes and subsequent acylation.
25 Additionally, TCVG excreted via the bile can be converted to TCVC in the intestinal
26 lumen and undergo entero-hepatic cycling (Hinchman and Ballatori, 1994; Irving and
27 Elfarrar, 2013).

28
29 The kidney is viewed as the main site for formation of genotoxic metabolites by β -lyase
30 cleavage of TCVC since β -lyase activity is relatively high in this organ. Smaller amounts
31 of β -lyase have been found in other organs, such as the liver, brain, and spleen
32 (Rooseboom, *et al.*, 2002), raising the possibility that reactive dichlorothioketene may be
33 generated and produce genetic damage in other tissues independent of its production in
34 the kidney. Although the liver contains a form of β -lyase, enzymatic cleavage of TCVC
35 does not appear to be significant in this organ. For example, in rats treated with the PCE-
36 conjugate analogues, dichlorovinyl glutathione (DCVG) and dichlorovinyl cysteine
37 (DCVC), significant pathology was observed in the kidney, but no tissue damage was
38 seen in the liver (Lash and Parker, 2001).

39
40 Oxidation of TCVC and N-AcTCVC to the reactive α,β -unsaturated sulfoxides can occur
41 in the liver and kidney, as well as other organs that contain flavin mono-oxygenase 3
42 (FMO3) or CYP450 3A activity. As noted above, the sulfoxides are reactive Michael
43 acceptors and can bond with nucleophilic sites on biological molecules. Discussing the

¹ Lymphocyte microsomes from male Wistar rats have been found to contain CYP450 2B, 2E, and 3A activity at 20, 4, and 2.4 percent of liver microsomal activity. Lymphocyte CYP450 content can also be chemically induced, resulting in 2 to 4-fold increases in activity (Hannon-Fletcher and Barnett, 2008).

1 metabolism of trichloroethylene (TCE), Irving and Elfarra (2012) noted that the α,β -
2 unsaturated sulfoxides formed in the GST pathway may be further conjugated with
3 glutathione, but that this process could also be reversible (by retro-Michael addition).
4 This would create a mechanism by which the reactive sulfoxides could circulate in a
5 stabilized form through the blood to other organs where they may be regenerated. The
6 mechanism would likely be operative for PCE as well.

7 8 Pharmacokinetic Model

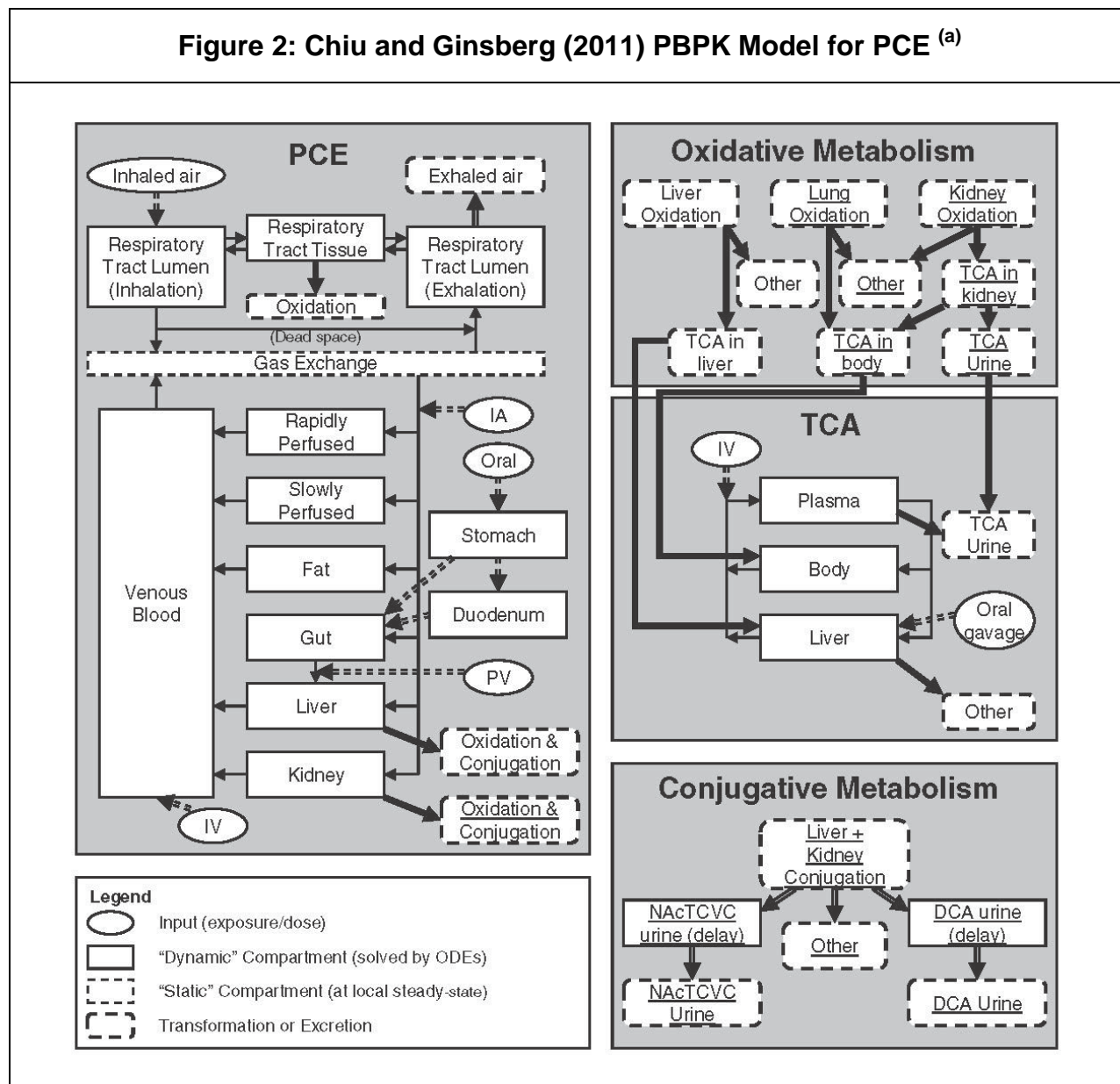
9 Numerous physiologically based pharmacokinetic (PBPK) models have been proposed
10 for PCE over the course of several decades. Reddy (2005), Clewell (2005), and US EPA
11 (2012a) have reviewed this body of research. Although the models are reasonably
12 consistent in estimating PCE blood concentrations, they differ widely in their predictions
13 of metabolized PCE at lower exposure concentrations. For example, at an inhaled
14 concentration of 1 ppb, some models predict about 1 or 2 percent metabolism, while
15 others predict metabolism in the range of 20 to 35 percent, and perhaps as high as 60
16 percent (Chiu and Ginsberg, 2011). Since PCE's carcinogenic potency is likely to depend
17 upon the formation of genotoxic metabolic products, the wide range of estimated PCE
18 metabolism among models has been a recognized problem for assessing the cancer risk
19 from low-level PCE exposure.

20
21 The most recent and comprehensive PBPK model for PCE is that of Chiu and Ginsberg
22 (2011). It was developed following the recommendations of the National Research
23 Council (NRC, 2010) that the available models for PCE be integrated into a single
24 harmonized model incorporating various improvements. The Chiu and Ginsberg (2011)
25 model incorporates lung, liver, kidney, fat, and venous blood compartments, and lumped
26 compartments for rapidly and slowly perfused tissues. It has components for simulating
27 inhalation, oral, and injection exposures. Absorption-desorption of PCE in the upper
28 respiratory tract (i.e., the "wash-in/wash-out" effect) is also taken into account. The rate
29 of PCE oxidation is modeled in liver, kidney and lung, and GSH conjugation is modeled
30 in the liver and kidney. The model can estimate (for example): concentrations of PCE in
31 exhaled air, blood concentrations of PCE and TCA, and urinary excretion of TCA and the
32 GSH-conjugation metabolites, N-AcTCVC and DCA. A graphical representation of the
33 Chiu and Ginsberg PBPK model is provided in Figure 2.

34
35 US EPA (2012) used the Chiu and Ginsberg (2011) model to estimate internal dose
36 metrics in its recent PCE cancer potency factor update, which included the development
37 of a URF for inhalation exposures. The most important improvements of the Chiu and
38 Ginsberg (2011) model, as discussed by the US EPA (2012a), are:

- 39
40 • It uses Bayesian Markov Chain Monte Carlo (MCMC) methodology to determine
41 the most likely values (posterior modes) for key metabolic constants.
- 42 • The model utilized all the available toxicokinetic data for PCE in mice, rats, and
43 humans, and is calibrated using a wide range of *in vivo* toxicokinetic data.

Figure 2: Chiu and Ginsberg (2011) PBPK Model for PCE ^(a)



(a) Figure adapted from Chiu and Ginsberg (2011). IV = intravenous, IA = intra-arterial, PV = portal vein.

- 1 • It is the first model to include a separate glutathione conjugation pathway.
- 2 • It incorporates recent information on TCA toxicokinetics from trichloroethylene
- 3 modeling studies.
- 4

5 Chiu and Ginsberg (2011) used a hierarchical Bayesian population approach to obtain
 6 estimates of the posterior modes² for a subset of important PBPK model parameters
 7 including: the pulmonary ventilation rate, metabolic constants for oxidation and
 8 conjugation of PCE, and urinary excretion of metabolites. Other model parameters, such

² These are also the maximum likelihood estimates (MLEs) since flat prior distributions were used in the model.

1 as partition coefficients and most of the physiological parameters, were fixed at baseline
2 values chosen from the literature. Inclusion of several intake routes (e.g., inhalation, oral,
3 and intravenous) allowed the model to be calibrated and evaluated against a wide variety
4 of experimental *in vivo* data.

5
6 In the MCMC analysis, sampling variation was characterized by running multiple chains
7 of length 5000 (retaining every 10th value) using randomly chosen starting conditions for
8 each chain. For the rodent PBPK models, 24 independent MCMC chains were run, each
9 producing a chain-specific, posterior mode estimate. The parameter set with highest
10 overall posterior probability of all the chains was selected as the posterior mode of the
11 optimized PBPK model. For the human model, 48 independent chains were used since
12 preliminary analysis indicated a potential for multiple maxima.

13
14 Table 1 shows a summary of predictions for several types of dose metrics based on the
15 optimized model for inhalation exposures, reported by Chiu and Ginsberg (2011). With
16 respect to the PCE AUC and PCE oxidation metrics, the range of chain-specific values
17 was less than 40% of the overall posterior mode estimates. For example, in the mouse
18 model at 1 ppm exposure, the overall posterior mode for percent of PCE oxidized was
19 17.4% of intake, and the range of chain-specific posterior modes was 11.5% to 17.9%.³

20
21 The estimates for PCE conjugation were more variable (with the exception of the rat
22 model). In mice exposed at 1 ppm, for example, the model predicts that 0.016% of PCE
23 intake will be conjugated with a range of 0.0068% to 0.43%. In the human model, the
24 overall posterior mode indicates that 9.4% of PCE intake is metabolized by GSH
25 conjugation, with a range of 0.003% to 10%. The human model displayed an apparent
26 bimodal distribution for the rate of GSH conjugation. Nonetheless, the most probable
27 posterior mode was at the high end of estimated conjugation rates.

28
29 Chiu and Ginsberg (2011) were not able to determine how much of the spread in the
30 human conjugation model was due to uncertainty or population variation, but noted that
31 the distribution could represent actual variability given the large differences in GST
32 activities displayed by humans. On the other hand, a high level of variability was not
33 observed in metabolic studies of trichloroethylene (TCE). Lash *et al.* (1999) looked at
34 rates of GSH conjugation of TCE in 40 ethnically and age-diverse, male and female
35 human liver samples and found less than a 10-fold variation.

36
37 As noted above, US EPA (2012a) used Chiu and Ginsberg's model results to derive its
38 updated PCE potency factors. However, because of the large range of model estimates
39 for PCE conjugation, US EPA prioritized the dose metrics based on oxidative metabolism
40 and PCE AUC in their final analysis.

³ Ranges of MCMC chain-specific posterior modes are from Table S-8 of Chiu and Ginsberg, 2011

Table 1: PCE Internal Dose Metrics from the Chiu and Ginsberg (2011) PBPK Model (and reproduced by the OEHHA model extract) ^(a) <i>Constant Inhalation Doses (posterior mode estimates)</i>						
Dose metric	Exposure Concentration (ppm)					Prediction Range (at 1 ppm)
	0.01	1	10	100	1000	
<i>PCE AUC Blood</i>	<i>(mg-hr)/(L-d) per ppm</i>					
Mouse	2.1	2.2	2.4	2.6	2.7	2.2-2.4
Rat	2.25	2.25	2.25	2.25	2.4	2.25-2.27
Human	2.0	2.0	2.0	2.0	2.0	2.0-2.4
<i>PCE Oxidation</i>	<i>Percent of intake that is oxidized</i>					
Mouse	18.8	17.4	11.8	7.3	6.6	11.5-17.9
Rat	4.2	4.2	4.1	3.3	1.1	3.9-4.2
Human	0.98	0.98	0.98	0.98	0.98	0.69-1.0
<i>PCE Conjugation</i>	<i>Percent of intake that is conjugated</i>					
Mouse	0.015	0.016	0.021	0.025	0.026	0.0068-0.43
Rat	0.31	0.31	0.31	0.32	0.335	0.20-0.50
Human ^(b)	9.4	9.4	9.4	9.4	9.3	0.003-10.0 (bimodal) ^(b)

(a) Values are from Chiu and Ginsberg (2011), Tables S-6 through S-8, and are also reproduced by OEHHA's inhalation-only model extract, at the presented level of significance.

(b) Values presented are for the most probable posterior mode.

1 *Use of Chiu and Ginsberg (2011) Harmonized PBPK Model*

2 Although there are unresolved issues related to the Chiu and Ginsberg model predictions
 3 for PCE's GST pathway, OEHHA considers the model to be the best available
 4 methodology for estimating dose metrics in the dose-response assessment. Regarding
 5 uncertainty in GSH conjugation, the Office evaluated the effect of including the GST
 6 pathway in the dose metric on the overall cancer potency analysis (see the following
 7 section).

8
 9 The full Chiu and Ginsberg (2011) model contains large portions of code designed to
 10 perform the Bayesian MCMC simulation, which determined the posterior mode estimates
 11 for key PBPK parameters. Once obtained, the posterior modes can be used to forecast
 12 the most likely values for internal doses at various exposure concentrations.

13
 14 For the inhalation potency evaluation, OEHHA relied on Chiu and Ginsberg's optimized
 15 PBPK model results. Since only dose metrics for inhalation exposures needed to be

1 estimated, the inhalation-relevant portion of the Chiu and Ginsberg (2011) model was
2 extracted. Specifically, OEHHA: (1) identified the main inhalation components of the MC-
3 Sim program obtained from the authors, (2) extracted the relevant equations and inputs
4 from the model code and translated them from the MC-Sim language into Berkeley
5 Madonna code, (3) ran the code using the optimized, Bayesian posterior mode
6 parameters and other baseline values developed by Chiu and Ginsberg (2011), and (4)
7 tested the output against the original model dose estimates reported in the Chiu and
8 Ginsberg (2011) paper.

9
10 A graphic depicting OEHHA's inhalation-only model is presented in Figure 3. As in the
11 original Chiu and Ginsberg model, it includes lung, liver, kidney, fat, and venous blood
12 compartments, and lumped compartments for rapidly and slowly perfused tissues. The
13 first transformation in the oxidative pathway is modeled in the lung, liver, and kidney, and
14 the first step of the GST pathway is included for liver and kidney. Absorption-desorption
15 of PCE in the upper respiratory tract is also included. The model adequately reproduced
16 the predictions of the original Chiu and Ginsberg model for inhalation exposures:
17 OEHHA's model extract reproduces the internal dose-metric values obtained by Chiu
18 and Ginsberg (2011), as presented in Table 1. The Berkeley Madonna model code for
19 mouse, rat, and human is provided in Appendix A.

20 21 Uncertainty and/or Variation in the Model Estimates

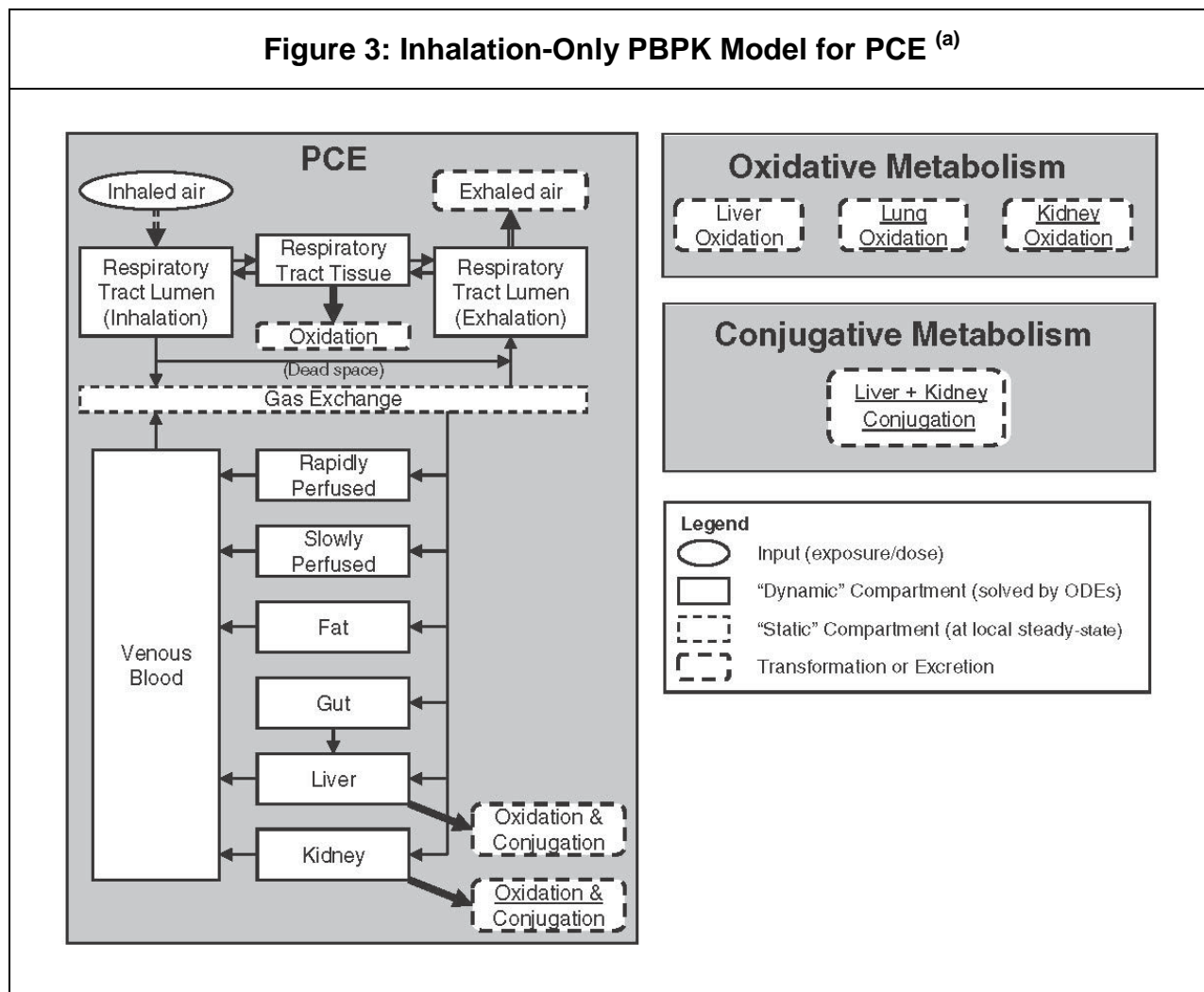
22 Additional discussion of the uncertainty related to GSH conjugation, particularly in the
23 human model, is provided here to support the choice of dose metric (presented later, in
24 Section 9). Three issues are addressed as follows.

25
26 First, as noted above, the modeled rate of GSH conjugation in humans displayed a
27 relatively high amount of uncertainty and/or variation: 0.003 -10%, with the overall
28 posterior mode at 9.4% of intake. Commenting on this large range, Chiu and Ginsberg
29 (2011) noted that the *in vivo* data available for model calibration were "inadequate to
30 constrain the flux through this pathway, either extreme providing plausible fits to the
31 data."

32
33 The overall posterior mode for PCE conjugation is, however, consistent with the *in vitro*
34 rates for TCE and other halogenated VOCs that have been reported in the literature
35 (e.g., Lash *et al.*, 1998; and Wheeler, *et al.*, 2001). The low value for PCE conjugation is
36 consistent with the low-end of *in vitro* activity obtained for PCE by Dekant *et al.* (1998),
37 which were below the analytical method detection limits.⁴

⁴ It should be noted that the *in vitro* GSH-conjugation data was not used to calibrate the model.

Figure 3: Inhalation-Only PBPK Model for PCE ^(a)



(a) Figure adapted from Chiu and Ginsberg (2011).

- 1 The large prediction range obtained in the human conjugation model raises a question -
- 2 particularly with regard to interspecies dose extrapolation - of whether the model's GSH
- 3 conjugation estimates should be used along with the PCE oxidation rates in a "total
- 4 metabolized dose" metric. The alternative would be to define an internal dose metric
- 5 using only the less-variable model predictions for PCE oxidation, as was done by US
- 6 EPA (2012a).⁵
- 7
- 8 The impact of PBPK model uncertainty in this case is muted when both PCE oxidation
- 9 and GSH conjugation are included together as a total metabolized dose, increasing the
- 10 potency estimate by about one order of magnitude (much less than the range observed
- 11 in the MCMC analysis).

⁵ Omitting GSH-conjugation from the internal dose metric is similar to using the lower-likelihood mode for human GSH-conjugation in a total metabolized dose. With the lower mode, the rates of conjugation for humans, rats, and mice would all be small relative to PCE oxidation rates, and thus have little impact on both the dose-response calculations using the rodent data and interspecies dose extrapolation using the human PBPK model.

1 In order to demonstrate this, OEHHA compared the results of interspecies dose
 2 extrapolation using the human PBPK model with the two alternative dose metrics, i.e.,
 3 using either total metabolism (GSH-conjugation + PCE oxidation) or PCE oxidation-only
 4 metabolism. We used the model to calculate human equivalent concentrations (HECs)
 5 from a range of example benchmark doses that could be obtained from the dose-
 6 response modeling of PCE exposure in rodents. As can be seen from the PBPK-derived
 7 HEC values presented in Table 2, the total metabolism dose metric produces HECs that
 8 are about 11-fold smaller than HECs obtained using an oxidation-only dose metric (Note
 9 that smaller HECs result in larger cancer potency factors).

10

Table 2: Impact of Internal Dose Metric Choice on Interspecies Conversion Calculations			
Example Benchmark Doses ^(a) (mg/kg-d)	PBPK-Derived Human Equivalent Concentration (HEC; ppm)		Ratio of HECs
	Oxidative + GSH Conjugation	Oxidative Metabolism Only	
0.1	0.61	6.5	10.7
1.0	6.1	65.0	
3.0	18.2	195.0	

(a) Since oxidative metabolism is significantly greater than GSH conjugation in rodents, both dose metrics will produce similar benchmark doses in the rodent dose-response models. A rough HEC comparison can therefore be made on a single benchmark dose for both dose-metric scenarios.

11 Thus, it appears that using a dose-metric incorporating a "high-end" value for human
 12 GSH conjugation, as opposed to using an oxidation-only dose metric which effectively
 13 sets GSH-conjugation to zero, adds a relatively small amount of "conservatism" to the
 14 dose-response analysis. OEHHA has determined that inclusion of the GST pathway in a
 15 total metabolized dose metric ensures that the resulting potency values are adequate to
 16 protect public health, per the recommendations of our current Air Toxics Hotspots
 17 program risk assessment guidelines (OEHHA, 2009).

18
 19 A second issue is whether using the model's uncertain estimate for glutathione
 20 conjugation in mice could have a large impact upon the dose-response calculation. As
 21 above, this question is addressed by looking at the difference between using either total
 22 metabolism or oxidation-only metabolism as the dose metric. In this case, the impact
 23 would be low. From Table 1, the model's posterior mode estimates of PCE oxidation and
 24 conjugation in mice indicate that oxidation dominates conjugation by factors of 290-1250,
 25 such that both dose metrics (total and oxidation-only) reflect mainly PCE oxidation, and
 26 should produce similar benchmark doses in a dose-response model.

1 Finally, there is an unresolved disagreement regarding the large variation in the results
2 of key *in vitro* studies that have estimated glutathione conjugation of PCE and TCE in
3 rodent and human tissues. In its IRIS PCE review, the US EPA (2012a) pointed out:

4
5 "The GSH pathway for tetrachloroethylene was originally demonstrated only in
6 rodents, and interpretation of the then-existing data led some scientists to
7 conclude that the pathway was not operative in humans (Green *et al.*, 1990).
8 More recent data clearly demonstrate the existence of the pathway in humans
9 (Schreiber *et al.*, 2002; Völkel *et al.*, 1998; Birner *et al.*, 1996) [...]

10
11 "There are discrepancies regarding reported rates of tetrachloroethylene GSH
12 metabolism (Lash *et al.*, 2007; Lash and Parker, 2001; Dekant *et al.*, 1998; Lash
13 *et al.*, 1998; Green *et al.*, 1990). These differences may be due, in part, to
14 different chemical assay methodology or to problems resulting from the stability of
15 the chemical product being measured or both (Lash and Parker, 2001)."

16
17 Some of the *in vitro* studies predict relatively high TCVG (and DCVG) production rates in
18 humans (e.g., Lash *et al.*, 1998; Lash *et al.*, 1999), while others indicate very low
19 conjugation. For example, with TCE, Green *et al.* (1997) measured DCVG formation at
20 0.19 picomole per minute per milligram protein (pmol/min/mg) using human liver cytosol
21 from 4 individuals. Conversely, Lash *et al.* (1999) measured TCE conjugation at 5,770
22 (pmol/min/mg) in human cytosolic protein pooled from 20 individuals. This large
23 difference in measured GSH conjugation rates is reflected in the uncertainty/variability
24 displayed by the Chiu and Ginsberg human model (and to a lesser extent, the mouse
25 model).

26
27 Several commentators have raised doubts regarding the accuracy of the PCE and TCE
28 conjugation rates reported by Lash *et al.* (1998, 1999, 2007), pointing to potential issues
29 with the chemical analysis methods used by the laboratory. On the other hand, the
30 apparent chemical instability of the GSH conjugates raises questions for studies that
31 have measured low conjugate levels. However, no work has apparently been done to
32 determine the true source of the discrepancy among the various divergent study results.
33 The Lash laboratory has published several papers following Lash *et al.* (1998) involving
34 the analysis of TCVG and DCVG, and has described various quality controls used
35 ensure analytical accuracy.⁶ Consistent results were generally obtained in these studies.
36 On the other hand, Lash, *et al.* (2006) measured DCVG levels in blood and tissue
37 samples of rats orally exposed to TCE and obtained a mixture of high and unexpectedly
38 low values. However, the higher values obtained by Lash *et al.* (2006) were generally
39 consistent with blood DCVG concentrations found in orally exposed mice by Kim *et al.*
40 (2009), and with mouse tissue and serum concentrations measured by Yoo, *et al.*
41 (2015), both using a different method of analysis.

42
43 Discrepancies in measured conjugation rates in humans might also be due to variable
44 quality of the tissue samples used, and it is possible that some samples were not
45 representative of the known variation in human GST activities. Thus, OEHHA does not

⁶ For example see, Lash *et al.* (2007) and Lash, *et al.* (1999).

1 find convincing evidence to discount the high-end *in vitro* values for human glutathione
2 conjugation of PCE, and estimated by the Chiu and Ginsberg (2011) PBPK model as
3 well.

4 5 **7. GENOTOXICITY AND CARCINOGENICITY**

6 Genotoxicity

7 A large number of studies have tested the genotoxicity of PCE, and less frequently its
8 metabolites, in microorganisms, mammalian cells, and in *Drosophila* and rodents. There
9 have also been a few occupational exposure studies looking at genetic abnormalities in
10 lymphocytes. This literature has recently been reviewed in detail by IARC (2014) and
11 US EPA (2012a). Selected results based on these reviews and the literature are
12 presented below.

13
14 PCE was not mutagenic in the Ames test with *S. typhimurium* or *E. coli* in the presence
15 or absence of S9 metabolic activation. It was mutagenic, however, in *S. typhimurium*
16 when tested with purified rat-liver GST, glutathione, and rat kidney fractions, where
17 TCVG would be formed (Vamvakas, *et al.*, 1989). Most studies looking at chromosomal
18 aberrations, micronuclei formation, or sister chromatid exchange have been negative,
19 but micronuclei induction was seen in Chinese hamster ovary cells (Wang *et al.*, 2001)
20 and human lymphoblastoid cells expressing CYP450 enzymes (White *et al.*, 2001).
21 Genetic alterations have also been observed in rapidly growing yeast cell cultures (US
22 EPA, 2012a).

23
24 Other types of tests, such as DNA strand break assays, DNA adduct and cell
25 transformation studies, and *Drosophila* mutation tests have provided mixed results.
26 Positive findings include: Elevated DNA single-strand breaks in mouse liver and kidney
27 *in vivo* (Walles, 1986), and DNA-adduct formation in mouse and rat tissues *in vivo*
28 (Mazzullo, *et al.*, 1987).

29
30 Results from occupational studies have also been mixed. Ikeda *et al.* (1980) tested ten
31 factory workers exposed to high (92 ppm PCE) or low (10-40 ppm) and found no
32 evidence of cytogenetic damage to lymphocytes or altered cell cycle kinetics. No
33 increase in sister chromatid exchanges in lymphocytes was found in a study of 27
34 subjects exposed to 10 ppm (geometric mean) of PCE (Seiji *et al.*, 1990). A decrease
35 (not increase) of 8-hydroxy-deoxyguanosine, a marker of oxidative DNA damage, was
36 observed in leukocytes of 38 female dry cleaners exposed to average concentrations of
37 less than 5 ppm PCE (Toraason *et al.*, 2003). On the other hand, a study of 18 dry-
38 cleaning workers exposed to 3.8 ppm PCE (average) found evidence of short-term
39 genetic damage to peripheral blood lymphocytes, indicated by an increase in acentric
40 chromosomal fragments (Tucker *et al.*, 2011).

41
42 Genotoxicity testing of various PCE metabolites includes the following positive results:

- 43
44 • TCA exhibited genotoxicity in several *in vivo* tests, for example: DNA strand
45 breaks, chromosomal abnormalities, and micronucleus formation in mice; and

- 1 chromosomal aberrations in chicken bone marrow (IARC, 2014; US EPA,
2 2012a).
- 3 • Genotoxicity has been demonstrated with DCA in the Ames test, micronucleus
4 induction test, a mouse lymphoma assay, and *in vivo* cytogenetic tests; DCA has
5 also been shown to cause DNA strand breaks *in vivo* in mouse and rat liver
6 (*ibid.*).
 - 7 • Trichloroacetyl chloride vapor tested positive in the Ames test with and without
8 metabolic activation (DeMarini, *et al.*, 1994).
 - 9 • PCE epoxide was mutagenic without metabolic activation in the Ames test with
10 *S. typhimurium* TA1535 at the lower doses tested; toxicity occurred at higher
11 doses (Kline *et al.*, 1982).
 - 12 • TCVG incubated with rat kidney protein containing γ -glutamyl transpeptidase
13 (GGT) and dipeptidases was mutagenic in the Ames test (Vamvakas, *et al.*,
14 1989).
 - 15 • TCVC and N-AcTCVC tested positive in the Ames test without metabolic
16 activation (Dekant *et al.*, 1986; Vamvakas, *et al.*, 1987).
 - 17 • TCVC sulfoxide was mutagenic in the Ames test with *S. typhimurium* TA 100, but
18 was 30-fold less potent than TCVC (Irving and Elfarra, 2013).

19
20 In addition, several metabolites have been tested for carcinogenicity in animals. Dermal
21 exposure of mice to PCE epoxide induced skin tumors (Van Duuren, *et al.*, 1983).
22 Several long-term drinking-water bioassays of TCA and DCA in mice, with limited
23 pathologic analysis of tissues other than the liver, found increases in hepatocellular
24 tumors. Initiation–promotion studies with TCA or DCA in mice also demonstrated that
25 they promote liver tumors following initiation by other carcinogens (IARC, 2014; Guyton
26 *et al.*, 2014).

27 Cancer Epidemiology

28
29 Numerous epidemiologic studies of PCE have been published, including more than 25
30 larger cohort and case-control studies since OEHHA's last toxicity review (*circa* 2000,
31 for our PHG for drinking water). Several detailed reviews of the literature have recently
32 been published (Guyton, *et al.*, 2014; IARC, 2014; and US EPA, 2012a).

33
34 Epidemiologic studies of PCE have all relied on semi-quantitative measures of exposure
35 such as high/medium/low, ever/never exposed, or job categories. As such, the exposure
36 data in this body of research are not of sufficient quality for use in quantitative dose-
37 response analysis. However, it provides evidence that PCE causes cancer in humans
38 and qualitatively supports the development of a unit risk value from animal studies. US
39 EPA (2012a) evaluated the results of the cohort and case-control studies that
40 developed more precise exposure assessments and concluded that PCE increases the
41 risk of three types of cancer in humans: bladder cancer, non-Hodgkin's lymphoma
42 (NHL), and multiple myeloma. IARC (2014) agreed with US EPA regarding bladder
43 cancer, but concluded that the evidence for PCE inducing other cancers in humans was

1 insufficient given the conflicting results across various studies. With non-Hodgkin's
2 lymphoma, for example, "three cohort studies showed an increased risk based on small
3 numbers, and the largest study with the best control of potential confounders did not.
4 Case-control studies on non-Hodgkin lymphoma did not find significant associations"
5 (*ibid.*).
6

7 A recent meta-analysis of bladder cancer risk in dry-cleaning workers (Vlaanderen, *et*
8 *al.*, 2014) integrated the results of seven studies and 139 exposed cases, and found an
9 overall relative risk level of about 1.5 for exposed versus non-exposed groups (with a
10 95% confidence level of 1.16 to 1.85).
11

12 Animal Studies of PCE

13 Increased tumor incidence was found in mice and rats in three long-term carcinogenicity
14 studies of PCE. An oral study was conducted by the National Cancer Institute
15 (NCI, 1977), where B6C3F₁ mice and Osborne-Mendel rats were administered PCE in
16 corn oil by gavage, 5 days/week for 78 weeks with additional follow-up of 32 weeks for
17 rats and 12 weeks for mice. PCE caused a significant increase of hepatocellular
18 carcinomas in mice of both sexes, and the tumors appeared considerably sooner in
19 treated mice than in controls. Survival in the high dose groups was much lower than the
20 control group at 40 to 45 weeks, and toxic nephropathy was observed in 93% of mice
21 exposed. In rats, a high level of early mortality occurred in all treated groups, which
22 obscured conclusions regarding carcinogenicity.
23

24 Two lifetime inhalation bioassays of PCE have also been published and are described
25 as follows.
26

27 A lifetime inhalation cancer study was conducted by the Japan Bioassay Research
28 Center (JBRC) of the Japan Industrial Safety and Health Association (JISHA, 1993).
29 Good Laboratory Practice (GLP) standards were used in the conduct of the study.
30 Dose-response data was analyzed by standard statistical procedures and study results
31 were thoroughly documented in a manner similar to NTP rodent cancer study reports.
32

33 The study was conducted using F344/DuCrj rats and Crj:BDF₁ mice. Groups of 50 male
34 and 50 female rats were exposed to PCE (99.0% pure) at 50, 200 or 600 ppm, and
35 similar groups of mice were exposed to 10, 50, or 250 ppm, for 6 hours per day, 5 days
36 per week, and 104 weeks. During the study period, the general status, body weight, and
37 food consumption of the animals were monitored. Urinalyses, hematological, and blood
38 chemistry tests were performed near the end of exposure for the surviving animals.
39 Upon death, animals were necropsied and organ weights were determined.
40 Histopathologic examination of all major tissue types was performed on all animals.
41 Survival was good for both sexes of rats and mice in all dose categories: more than 80
42 percent of rats and 70 percent of mice were alive at week 92. Nonetheless, survival was
43 significantly reduced at the highest exposure levels when compared with control groups.

1 Additional findings related to tumorigenesis are (see also Table 3):
2

- 3 • For exposed male and female rats, the only tumor type that was found to be
4 elevated was mononuclear cell leukemia (MCL). A statistically significant dose-
5 response trend was found by the Cochran-Armitage and exact trend tests (in
6 males) or a life-table test (in females). In addition, for males, the highest dose
7 category displayed a significant increase when compared to controls by the
8 Fisher exact test.
9
- 10 • In exposed mice, an increased incidence of hepatocellular adenoma and
11 carcinoma was found in both sexes as indicated by significant dose-response
12 trends and pair-wise comparison of the high dose category against controls. In
13 the males, there was also an increase in all-organ, hemangioma or
14 hemangiosarcoma (mostly in the spleen and liver), and Harderian gland tumors.
15

16 NTP (1986) conducted a study where B6C3F1 mice and F344/N rats, in groups of 50,
17 were exposed to PCE (99.9% pure) by inhalation, 6 hours/day, 5 days/week for 103
18 weeks. Mice were exposed to concentrations of 100 or 200 ppm, and rats to 200 or 400
19 ppm, in addition to controls. The general status and body weight of the animals were
20 monitored during the study. Upon death, animals were necropsied and histopathologic
21 examination of all relevant tissues was performed on all animals. Approximately 70
22 percent or more of both sexes of mice and rats were alive at week 90 of the study.
23 Survival was significantly reduced in male rats at the higher exposure level when
24 compared with controls. Survival was decreased in both dose levels in male mice and in
25 the high dose group of female mice.
26

27 As shown in Table 4, PCE significantly increased the rate of hepatocellular carcinomas
28 in mice of both sexes. The combined incidence of liver adenoma or carcinoma was also
29 increased, although the incidence of liver adenomas separately was not. In female and
30 male rats, PCE also produced significant increases in mononuclear cell leukemia
31 (MCL). Male rats additionally exhibited apparent increases in tumor incidence in the
32 kidney, brain, and testes. Statistical tests for increases in renal tubular-cell adenomas
33 and adenocarcinomas appeared to be dose-related, but did not reach customary
34 significance levels. However, the historical incidence of these tumors is low (0.4%) at
35 the laboratory and increased incidence has been found with other chlorinated ethanes
36 and ethylenes. Thus renal tubular-cell tumors were judged to be related to PCE
37 exposure. Brain glioma, another rare tumor type in F344 rats, was observed in one male
38 control rat and in four male rats at 400 ppm exposure. This increase was not statistically
39 significant. However, because the historical incidence of these tumors is 0.8% for the
40 laboratory, the increased brain tumor incidence in this study was also carried through the
41 analysis. Testicular interstitial cell tumors showed significant dose-responses in both life
42 table and incidental tumor tests calculated by NTP. This tumor type was therefore
43 included in the dose-response evaluation, but was considered to be more uncertain,
44 given the high background rate of testicular tumors in F344 rats (both historically and in
45 the NTP study controls).

Table 3: Primary Tumor Incidence in Mice and Rats Exposed to PCE Rates at Exposure Concentrations in PPM (JISHA, 1993)									
Mice (Crj:BDF₁)									
Tumor Type	Sex	Adjusted Rates ^{(a)(b)} (at 0-250 ppm)				Rate Percent (at 0-250 ppm)			
		0	10	50	250	0	10	50	250
Hepatocellular adenoma or carcinoma	M	13/46**	21/47	19/47	40/49**	28.3	44.7	40.4	81.6
	F	3/44**	3/41	7/40	33/46**	6.8	7.3	17.5	71.7
Hemangioma or hemangiosarcoma (All sites)	M	4/46*	2/47	7/47	9/49*	8.7	4.3	14.9	18.4
Harderian gland adenoma	M	2/41**	2/45	2/37	8/39	4.9	4.4	5.4	20.5

Rats (F344/DuCrj)									
Tumor Type	Sex	Adjusted Rates ^{(a)(b)} (at 0-600 ppm)				Rate Percent (at 0-600 ppm)			
		0	50	200	600	0	50	200	600
Mononuclear cell leukemia	M	11/50**	14/48	22/50	27/49*	22.0	29.2	44.0	55.1
	F	10/50 ^(c)	17/50	16/50	19/50	20.0	34.0	32.0	38.0

(a) Tumor-incidence denominator adjusted by excluding animals dying before the first corresponding tumor type observed in each study.

(b) Statistical test indicators: (*) P-value < 0.05; (**) P-value < 0.005. Fisher exact test results are as reported by JISHA, except that mouse, all-site hemangioma/hemangiosarcoma values were calculated by OEHHA. The control group column indicates the results of trend tests. Both the Cochran-Armitage trend test (reported by JISHA) and the exact trend test calculated by OEHHA gave the same indications of significance.

(c) A significant trend was found in a life-table test reported by JISHA, P-value = 0.049.

Table 4: Primary Tumor Incidence in Mice and Rats Exposed to PCE Rates at Exposure Concentrations in PPM (NTP, 1986)							
Mice (B6C3F₁)							
Tumor Type	Sex	Adjusted Rates ^{(a)(b)} (at 0-200 ppm)			Rate Percent (at 0-200 ppm)		
		0	100	200	0	100	200
Hepatocellular adenoma or carcinoma	M	17/49**	31/47**	41/50**	34.7	70.0	82.0
	F	4/44**	17/42**	38/47**	9.1	40.5	80.9

Rats (F344/N)							
Tumor Type	Sex	Adjusted Rates ^{(a)(b)} (at 0-400 ppm)			Rate Percent (at 0-400 ppm)		
		0	200	400	0	200	400
Mononuclear cell leukemia	M	28/50*	37/48*	37/50*	56.0	77.1	74.0
	F	18/49*	30/50*	29/50*	36.1	60.0	58.0
Renal tubule adenoma or carcinoma	M	1/47 ^(c)	3/42	4/40	2.1	7.1	10.0
Brain glioma	M	1/44 ^(c)	0/37	4/35	2.3	0.0	11.4
Testicular interstitial cell	M	35/49 ^(c)	39/46	41/50	71.4	84.8	82.0

(a) Tumor-incidence denominator adjusted by excluding animals dying before the first corresponding tumor type observed in each study.

(b) Statistical test indicators: (*) P-value < 0.05; (**) P-value < 0.005. Fisher exact test results are as reported by NTP. The control group column indicates the results of trend tests. Both the Cochran-Armitage trend test (reported by NTP) and the exact trend test calculated by OEHHA gave the same indications of significance.

(c) Although testicular tumors and brain glioma did not appear to be significantly increased by the Fisher exact and trend tests, life table tests conducted by NTP did show significant increases in trends of <0.001, and 0.039 respectively. In addition, NTP's incidental tumor tests showed increased testicular tumors by both trend and pair-wise comparisons. The life table trend test for kidney tumors was nearly significant at 0.054.

1 Primary Studies for the Dose-Response Assessment

2 Both the NTP (1986) and JISHA (1993) inhalation studies were judged to be of high quality
3 and suitable for the development of an inhalation potency factor. The studies used different
4 strains of mice (Crj:BDF₁ vs. B6C3F₁) and different substrains of F344 rats. They displayed
5 variability of outcome with respect to the tissues affected, as well as the strength of the
6 dose-response relationships for various tumor types, and differing incidence rates in the
7 control groups. Some of this variability could be due, in the case of the rat models, to the
8 fact that the different substrains used may have genetic and phenotypic variation as a
9 result of mechanisms such as genetic drift.

10
11 For example, Tiruppathi *et al.* (1990) and Thompson *et al.* (1991) reported that the
12 Japanese and German substrains of the Fischer 344 (F344) rat, but not the US substrain,
13 were deficient in dipeptidyl dipeptidase-4 activity in the kidney and liver. This enzyme has
14 been implicated in the degradation of collagen, blood clotting, immunomodulation, and
15 metabolism of hormonal peptides (Tiruppathi, *et al.*, 1990). While this particular enzymatic
16 variation may not be directly relevant to PCE metabolism, it indicates that F344 rat
17 substrains can display significantly divergent biological traits. With regard to the mice, the
18 genetic variation issue is accentuated by the use of two different mouse hybrid strains, not
19 substrains.

20
21 Although it cannot be determined whether the different outcomes for mice and rats
22 observed by NTP (1986) and JISHA (1993) resulted from differences in animal biology, the
23 data suggest that each study provides non-redundant information for the analysis.

24
25 The JISHA dataset offers the advantage of an additional dose category for each species,
26 as well as the use of several lower exposure concentrations. Moreover, the control rate of
27 MCL incidence in the F344/DuCrj rats used in the Japanese study (22 and 20%) was
28 significantly lower than for the F344/N rats used in the NTP study (56 and 36%), and is
29 expected to improve the precision of the fitted model. The NTP study, nonetheless,
30 provides important additional data on tumor development in the kidney, brain, and testes of
31 F344/N rats, and supporting data on the dose-response rate for MCL.

32
33 Based on the above considerations, OEHHA chose both the JISHA (1993) and NTP (1986)
34 bioassays as primary studies for the dose-response analysis. The dose-response data and
35 results of statistical tests are presented in Tables 3 and 4. Given the availability of two
36 acceptable inhalation studies, the oral NCI (1977) study was not used in the quantitative
37 analysis.

38
39 Relevance of MCL to Humans

40 Some concerns about the propriety of using the rat MCL data for human risk assessment
41 were raised by an NRC expert panel (without consensus) during a review of US EPA's
42 PCE IRIS evaluation (NRC 2010). One issue brought up by the panel was that MCL is a
43 common tumor in aging F344 rats that lacks a corresponding tumor in humans. Panel
44 members also questioned the statistical significance of the MCL dose-response data in
45 light of the elevated historical and control-group incidence rates for MCL. This section
46 briefly addresses both questions.

47
48 Regarding the issue of tumor-site concordance, current research in cancer biology

1 indicates that the basic cellular mechanisms of carcinogenesis are similar among
2 mammals. However, this does not imply that exposure to a chemical carcinogen will
3 always produce cancer in the same organ in different species (US EPA, 2005). In the
4 case of human leukemias and lymphomas that are known to be induced by specific
5 carcinogens, rodents develop different types of leukemia and lymphoma (US EPA,
6 2012c). The sites of induced cancer may not be the same because of differing
7 toxicokinetics and tissue susceptibilities. For leukemia and lymphoma, variation in
8 susceptibility could be related to differences in hematopoiesis and immune surveillance.
9 Accordingly, there is no expectation—in general or specifically for MCL—of tumor-site
10 concordance when using animal studies to predict human cancer risk (OEHHA, 2009).

11
12 Notwithstanding this general principle, there is evidence that rat MCL corresponds to at
13 least one form of human leukemia. The specific cell type and biological mechanisms that
14 give rise to rat MCL are not known, but it appears to arise from a lymphocyte or monocyte
15 lineage, and it is thought that the cell of origin resides in the spleen or undergoes
16 neoplastic transformation in the spleen (Thomas *et al.*, 2007). One reasonable hypothesis
17 is that rat MCL is a form of Large Granular Lymphocyte Leukemia (LGLL), a cancer that
18 develops in the spleen and is phenotypically and functionally similar to human LGLL
19 (IARC, 1990; Thomas *et al.*, 2007). Human LGLL derives from either T-cell or natural killer
20 (NK) cell lineages (Sokol and Loughran, 2006). Additional support for linking rat MCL to
21 human LGLL is provided by a study using the F344 rat MCL as a model for human NK-
22 LGLL, which observed similar cellular responses in samples of the two tumor-cell types
23 (Liao *et al.*, 2011).

24
25 Exposure of humans and animals to relatively low doses of PCE produces adverse effects
26 upon blood and the immune system (e.g., see: Marth, 1987; Kroneld, 1987; and Emara *et*
27 *al.*, 2010) that could plausibly give rise to a variety of carcinogenic response in different
28 species. In addition to human LGLL, rat MCL may correspond to other types of human
29 leukemia or lymphoma.

30
31 Regarding statistical issues arising from the elevated incidence of MCL in control groups,
32 an NTP workshop focusing on the high background incidences of MCL and other tumors
33 in the F344 rat noted that, “From a statistical perspective, high background rates of such
34 tumors in control animals will generally decrease the ability to detect an exposure-related
35 effect. In addition, when a statistically significant tumor effect is found in test animals
36 relative to concurrent controls, the effect may not be considered exposure-related if it falls
37 within the range observed in historical controls” (King-Herbert and Thayer, 2006). The
38 foregoing statement focuses on the problem of false negative test results. However, since
39 US EPA found MCL incidence to be significantly elevated in PCE-exposed rats, NRC
40 panel members were concerned with the potential for false positive test results. On this
41 issue, OEHHA agrees with the Massachusetts Department of Environmental Protection
42 (MDEP), who reviewed the historical background rates of MCL in the NTP and JISHA
43 study laboratories and found that,

44
45 "For both the NTP (1986) and JISHA (1993) studies, the background rate of MCL in
46 the same study control group was greater than or equivalent to the historical control
47 rates for the same lab, same sex. Thus, the controls in both studies did not exhibit

1 anomalously low MCL, which could, had it occurred, lead to false positive responses in
2 the treatment groups." (MDEP, 2014)

3
4 Indeed, for the JISHA male rat MCL data, where the incidence in study controls was 22%,
5 the historical incidence was 6-22%, and the Cochran-Armitage test for trend was highly
6 significant, having a p-value of less than 0.0005.

7 8 **8. MODE(S) OF ACTION**

9 PCE's carcinogenic modes of action (MOA) likely involve the genotoxicity of one or more
10 of its oxidative- or GST-pathway metabolites, although the precise mechanisms are
11 unknown.

12
13 Several PCE metabolites, e.g., PCE epoxide, oxalyl chloride, trichloroacetyl chloride,
14 dichlorothioketene, and the TCVC sulfoxides, are reactive compounds and expected to
15 have short half-lives in the nucleophile-rich cellular environment.⁷ These substances will
16 tend to react chemically and enzymatically with cellular components near their site of
17 production. The relatively stable metabolites, such as: TCA, DCA, TCVC, and N-AcTCVC,
18 are more likely to circulate throughout the body where they may be further metabolized
19 and impact tissues other than the liver and kidney.

20
21 Both trichloroacetic acid (TCA) and dichloroacetic acid (DCA) have independently been
22 found to increase tumor formation in mice. Since TCA is a major metabolite of PCE, US
23 EPA (2012a) evaluated whether it could be the primary source of PCE's carcinogenicity in
24 mouse liver. Using dose-response data from the JISHA (1993) and NTP (1986) PCE
25 studies and a drinking water study of TCA in mice (DeAngelo, *et al.*, 2008), US EPA found
26 that metabolically-generated TCA could contribute from 12 to 100 percent of the
27 increased risk of liver tumors. This large range is not highly informative, and leaves open
28 the possibility that other reactive metabolites may contribute significantly to the production
29 of liver tumors in mice.

30
31 There are several non-genotoxic MOAs that may contribute to PCE's carcinogenicity,
32 though in as yet poorly understood ways. These have been discussed at length by US
33 EPA (2012a), and include: cytotoxicity with subsequent cellular proliferation, oxidative
34 stress-induced cellular transformation, and dysregulation due to altered DNA methylation.
35 Two specific MOAs that are potentially relevant for evaluating PCE involve α 2u-globulin
36 nephropathy in the male rat, and PPAR α activation⁸ for mouse liver tumors. In both cases,
37 the biological bases for these MOAs in rodents are thought to be muted or absent in
38 humans, indicating that the particular tumor-types may not be useful for human risk
39 assessment.

40 41 *α 2u-Globulin Nephropathy*

42 The α 2u-globulin MOA in male rats is defined by: accumulation of α 2u-globulin-containing
43 hyaline droplets in the proximal tubules of the kidney, cytotoxicity with tubular cell
44 proliferation, exfoliation of epithelial cells into the proximal tubular lumen and formation of

⁷ For example, the high reactivity of PCE epoxide is indicated by its 2.6-minute half-life in a neutral aqueous buffer solution at 37 °C (Yoshioka, *et al.*, 2002).

⁸ PPAR α = "peroxisome proliferator-activated receptor- α ."

1 granular casts, papillary mineralization, hyperplastic foci, and renal tumors (US EPA,
2 1991).

3
4 Green *et al.* (1990) found accumulation of α 2u-globulin in the proximal tubules of F344
5 rats exposed by inhalation to 1000 ppm of PCE for 10 days, or given 1500 mg/kg PCE by
6 gavage for 42 days. However a 400 ppm inhalation exposure for 28 days did not produce
7 protein droplets or other signs of toxicity. For chemicals known to cause α 2u-globulin
8 toxicity, the formation of protein droplets in the kidney occurs rapidly upon exposure
9 (frequently after a single dose), and further indications of tissue damage begin to appear
10 in 3 to 4 weeks (Lehman-McKeeman, 2010; Green *et al.*, 1990). Thus, the absence of
11 α 2u-globulin accumulation after a 28-day exposure suggests that 400 ppm of PCE will not
12 result in α 2u-globulin toxicity upon long-term exposures.

13
14 The NTP (1986) study provided additional evidence along these lines. Karyomegaly and
15 cytomegaly were observed in the kidneys of rats exposed to 200 or 400 ppm for 2 years,
16 but indicators of α 2u-globulin nephropathy (e.g., hyaline droplets, mineralization, and cast
17 formation) were not found. The NTP protocol at the time was not designed to detect
18 hyaline droplets or α 2u-globulin accumulation (US EPA 2012a) but would have observed
19 other markers of α 2u-globulin toxicity if this MOA had been in effect. Moreover,
20 comparable toxicity was observed in female rats in the NTP study, and PCE caused
21 similar kidney damage in rats and mice of both sexes in the NCI (1977) gavage study.
22 This suggests that PCE's nephrotoxicity is neither sex nor species specific, as would be
23 expected with an α 2u-globulin MOA.

24 25 PPAR α Activation

26 The PPAR α MOA involves activation of the PPAR α nuclear receptor, which is
27 hypothesized to cause alterations in cell proliferation and apoptosis, and clonal expansion
28 of initiated cells. The proposed indicators for this mode of action are: (1) PPAR α activation
29 with associated peroxisome proliferation, or (2) PPAR α -activation plus increased liver
30 weight and effects such as increased peroxisomal β -oxidation, CYP4A, or acyl CoA
31 oxidase (Klaunig, *et al.*, 2003).

32
33 Numerous studies have been carried out to verify the PPAR α MOA. The evidence
34 obtained from this body of research has been mixed, and it currently remains unclear
35 whether this hypothetical MOA is a major causal factor in mouse-liver tumor formation.
36 The US EPA has published several detailed reviews of the PPAR α MOA in its IRIS
37 program toxicity reviews for PCE and TCA (US EPA 2012a, 2011). The main conclusions
38 of these reviews are:

- 39
- 40 • PPAR α activators can produce multiple effects in addition to peroxisome
41 proliferation, including genotoxicity, oxidative stress, hypomethylation of DNA, and
42 activation of other nuclear receptors.
 - 43 • Peroxisome proliferation and the associated markers of PPAR α activation are poor
44 predictors of hepatocarcinogenesis in mice and rats. Studies with various PPAR α
45 activators show that the correlation between *in vitro* PPAR α activation potency and
46 tumorigenesis is weak and this relationship does not appear to be due to

1 differences in pharmacokinetics. This suggests the involvement of carcinogenic
2 mechanisms other than PPAR α -activation.

- 3 • Studies of the PPAR α -agonist, diethyl hexyl phthalate (DEHP) in transgenic mouse
4 strains, although not fully conclusive, have cast doubt on whether the key events in
5 the PPAR α MOA (receptor activation, hepatocellular proliferation, and clonal
6 expansion) are sufficient to cause liver tumors. The studies suggest that DEHP can
7 induce tumors in a PPAR α -independent manner (Ito *et al.*, 2007a), and that PPAR α
8 activation in hepatocytes is insufficient to cause tumorigenesis (Yang *et al.*, 2007).
9 This again indicates that other mechanisms, either independently or in combination
10 with PPAR α -activation, are necessary to induce tumors.
- 11 • PCE exposure leads to PPAR α -activation and modest levels of peroxisome
12 proliferation, predominantly through its metabolite TCA. There is conflicting
13 evidence as to whether this causes cellular proliferation in animals exposed to
14 PCE: the peroxisome proliferation caused by PCE lacks specificity and consistency
15 with respect to tissue, species, dose, and sequence of events. Also, there is little
16 evidence indicating that PCE can induce clonal expansion of initiated cells. The
17 available information for PCE is insufficient to demonstrate that the PPAR α MOA
18 plays a significant causative role in mouse hepatocarcinogenesis.

19 Conclusion on PCE's Mode(s) of Action

21 Given the limited understanding of the various non-genotoxic MOAs that may modify or
22 add to the tumorigenic effects of PCE's genotoxic metabolites, there are insufficient
23 grounds to evaluate PCE as primarily a non-genotoxic carcinogen using a non-linear
24 model.

25 **9. DOSE-RESPONSE ASSESSMENT**

26 Dose Metrics

28 Much of the following information has already been presented, but is briefly restated here
29 because of its relevance to choosing metrics for the dose-response calculations:

- 31 • The liver is the main site of oxidative PCE-metabolite formation, but other tissues
32 with CYP 450 2E1, 2B, and 3A activity may also contribute to the oxidative-
33 pathway. TCA is a relatively stable metabolite that has been found to increase liver
34 tumors in mice via oral exposure. TCA's cancer potency in other tissues has not
35 been adequately examined.
- 36 • Of the two metabolic pathways, oxidation is the main pathway in rodents. For
37 example, at 10 ppm exposure, the PBPK model indicates that the ratio of oxidation
38 to glutathione conjugation is 600 in mice and 19.5 in rats.
- 39 • Saturation of the oxidative pathway begins to occur between 1 and 10 ppm
40 exposure in mice, and between 10 and 100 ppm exposure in rats (see Table 1).
41 Saturation causes the ratio of oxidized to absorbed PCE to decrease at higher
42 exposure concentrations. The smaller amount of metabolism that occurs via the
43 GST pathway, on the contrary, increases somewhat at higher exposure
44 concentrations in rodents.

- 1 • Although most GST conjugation of PCE takes place in the liver, the kidney is likely
2 to be the main site for production of reactive GST-pathway metabolite
3 dichlorothioketene. Other metabolites such as: TCVC, N-AcTCVC, and TCVC
4 sulfoxide are formed in both the liver and kidney, and may circulate to other
5 metabolizing tissues as well.
- 6 • It is not known which PCE metabolites, or even which of the two main metabolic
7 pathways produces the most carcinogenic risk.
- 8 • The PBPK model for the GST pathway in humans involves a large variability or
9 uncertainty, with two possible values (posterior modes) for the rate of PCE
10 conjugation that differ by a factor of approximately 3000. However, as was
11 discussed earlier in Section 6, the impact of the human PBPK model
12 uncertainty/variability upon the overall dose-response evaluation is several orders
13 of magnitude lower than this. It is not known how much of the model variability is
14 due to the wide range of GST activities that have been observed in the human
15 population, but it is reasonable to assume that some segment of the population
16 could be efficient metabolizers while other segments (e.g., individuals who are
17 homozygous in GST-null variants) could be much less efficient. It is currently
18 unclear which GST isoforms are most active with regard to PCE conjugation.
- 19 • The more probable and larger of the two values indicates that glutathione
20 conjugation predominates over oxidation in humans, the ratio of PCE conjugation
21 to oxidation being about 10.

22
23 OEHHA considered the advantages and disadvantages of using several dose metrics for
24 the dose-response calculations. These are briefly discussed below.

- 25
26 • Applied air concentration: This would be the simplest approach in that it does not
27 rely upon the output of complicated PBPK modeling calculations. However, given
28 the large body of evidence indicating that PCE's metabolites are likely to be
29 responsible for its tumorigenic properties, using applied concentration as the dose
30 metric may reduce the accuracy of the dose-response analysis, especially for the
31 mouse, where the dose-response data indicate significant metabolic saturation in
32 the oxidative pathway at the higher PCE exposure concentrations tested.
- 33
34 • PCE blood concentration: This dose metric does make use of the PBPK modeling
35 estimates but has the same weakness as using the applied air concentration, since
36 blood concentrations of the parent compound may not be directly related to
37 concentrations of the potentially carcinogenic metabolites of PCE. Blood
38 concentrations of PCE may even be less accurate than applied concentrations,
39 since PCE blood concentrations are expected to be inversely related to metabolite
40 concentrations (For example, see Table 1 entries for the mouse dose-metrics
41 where "PCE AUC per ppm exposure" increases and "percent oxidation/ppm"
42 decreases) as one moves to higher exposure concentrations).
- 43
44 • Pathway specific metabolized dose: Defining a dose metric based upon either the
45 oxidation or GST conjugation pathway would be better in terms of focusing on the
46 production of PCE's carcinogenic metabolites instead of the parent compound.

1 However, using either of the two pathways alone would be problematic, since each
2 pathway produces several genotoxic substances that could be important for PCE's
3 overall tumorigenicity. From Table 1 it can be seen that for mice, the quantity of
4 oxidative metabolites produced with increasing exposure appears to be inversely
5 related to the quantity of conjugation metabolites. Furthermore, if humans are more
6 efficient conjugators than rodents, using an oxidation-only dose metric could
7 underestimate the dose-response function. On the other hand, using glutathione
8 conjugation alone has the problem of large model uncertainties with larger impacts
9 upon the overall dose-response assessment (note that this impact is muted for total
10 metabolism, as discussed above in Section 6).

- 11
12 • Choosing one or more metabolites: Using a subset of concentrations of one or
13 more metabolites for the dose metric has similar problems as using pathway
14 specific metabolism. For example, in Section 8 we briefly discussed US EPA's
15 evaluation of TCA, a major metabolite generated in the oxidation pathway, where it
16 was estimated that TCA might be responsible for as little as 12 percent of liver
17 tumor risk in mice. An added issue is that the available PBPK models only
18 incorporate a few of the various metabolites, such as TCA and DCA.
- 19
20 • Total PCE metabolized dose: Using total metabolism for the dose metric accounts
21 for toxicokinetic differences across species and provides a dose adjustment for
22 saturation effects in the oxidative pathway. It has the advantage of taking into
23 account both pathways generating potentially carcinogenic metabolites. However, it
24 involves assuming that carcinogenic potency is proportional to the combined rate of
25 the first step of metabolism in each pathway. This assumption is simplistic but
26 unavoidable given the many unknowns involved in PCE's toxicokinetics and
27 toxicodynamics. As noted above, total metabolized dose has an advantage over
28 using either oxidative or glutathione conjugation alone. Using oxidation-only may
29 not be adequately protective of human health given the potential genotoxicity of
30 metabolites formed in the conjugation pathway. Total metabolized dose is also
31 advantageous compared with using the GST-pathway metabolites alone, since the
32 PBPK modeling uncertainties have relatively little impact upon the dose-response
33 assessment using total metabolism as the metric.

34
35 Considering all of the above factors, total metabolism was chosen as the best dose metric
36 for the dose-response analysis of all the tumor types identified in the primary mouse and
37 rat studies.⁹ The PBPK-estimated, total metabolized doses used in the dose-response
38 analysis are presented in Appendix B.

39 Dose-Response Model

40 Based upon its metabolic profile and the genotoxic activity of some of the metabolites
41 formed, OEHHA considers PCE to be a genotoxic carcinogen. This information supports
42 the assumption that the dose-response relationship approaches linearity at low doses and

⁹ In using total metabolized dose as the preferred dose metric, OEHHA considered the uncertainty in the available scientific information and, in contrast to US EPA (2012a), has chosen a modeling approach that will produce a more health-protective potency estimate. This is consistent with OEHHA's cancer risk assessment guidelines (OEHHA 2009), which establish a policy of developing cancer potency factors that are adequate to protect public health.

1 the use of the multistage cancer model to estimate the potency factor. This is consistent
2 with OEHHA risk assessment guidelines, which indicate that use of the multistage model
3 (and assuming low-dose linearity) is reasonable under such circumstances (OEHHA,
4 2009). In the traditional, linearized-multistage model, cancer potency is estimated as the
5 upper 95% confidence bound, (q_1^*), on the linear coefficient (q_1) in the following expression
6 relating lifetime probability of cancer (p) to dose (d):

$$p = q_0 + (1 - q_0)(1 - \exp[-(q_1d + q_2d^2 + \dots)])$$

8
9 In the above equation, (d) represents the average daily dose resulting from a uniform,
10 continuous exposure over the nominal lifetime of the animal (two years for both mice and
11 rats); (q_0) is the tumor incidence in the non-exposed group. For studies where the
12 exposures vary in time, they are averaged over the entire study period and modeled as if
13 they were uniform and continuous. Prior to fitting the dose-response model to the study
14 data, an adjustment is made to the incidence rates to account for inter-current mortality,
15 which decreases the pool of animals at risk of developing tumors throughout the study.

16
17 The latest version of BMDS (Version 2.6.0.1, US EPA, 2015) was used to carry out the
18 necessary dose-response calculations. The BMDS dichotomous multi-stage cancer model
19 was run for all allowed degrees of the approximating polynomial, with a benchmark risk
20 (BMR) of 5 percent. Instead of (q_1^*) the software calculates benchmark doses (BMDs) and
21 their 95% lower confidence levels (BMDLs). When multiplied by the BMR, the reciprocal of
22 the BMDL gives a unit risk factor that is generally close in value to, and is used in place of
23 (q_1^*). For each tumor site, the model with the lowest value of AIC (Akaike's Information
24 Criterion) was chosen, as long as its p-value for goodness-of-fit was above 0.1 and the
25 absolute value of the scaled residual for the dose near the BMD was less than 2.0. The
26 optimal model typically resulted from fitting a polynomial of 1 or 2 degrees, and the models
27 with the lowest AIC also had the highest p-values (signifying the best fit to the data).

28
29 Interspecies extrapolation from experimental animals to humans was based on body
30 weights (bw) raised to three-quarters power (US EPA, 2005; Anderson *et al.*, 1983), which
31 for BMDLs, may be expressed in terms of body weight raised to one-quarter power, as
32 follows:

$$BMDL_{(Human)} = BMDL_{(Animal)} \times \left(\frac{bw_{(Animal)}}{bw_{(Human)}} \right)^{1/4}$$

33 The above equation is presumed to account for the toxicokinetic and toxicodynamic
34 differences between species. Toxicokinetic modeling can sometimes eliminate the need for
35 toxicokinetic scaling between animals and humans. This would be the case, for example, if
36 the dose metric used in the analysis was the AUC of a directly carcinogenic metabolite.
37 The remaining toxicodynamic differences would then be addressed, according to OEHHA
38 practice, by scaling according to the one-eighth power of the body weight ratio.¹⁰ Using the
39 rate of PCE metabolism as a dose metric, on the other hand, does not account for the
40 toxicokinetics of other downstream biological processes that determine tissue
41 concentrations of the relevant carcinogenic species. In this case, the full cross-species

¹⁰ US EPA risk assessment guidelines (2005) suggest "retaining some of the cross-species scaling factor (e.g., using the square root of the cross-species scaling factor)," when toxicokinetic modeling is used without toxicodynamic modeling.

1 scaling factor is used (US EPA, 1992).

2
3 Since PCE induced tumors at multiple sites in male mice (JISHA study) and male rats
4 (NTP study), the combined cancer potency was also estimated for these groups using the
5 multi-site tumor module provided in BMDS. The BMDS procedure for summing risks over
6 several tumor sites uses the profile likelihood method. In this method, the maximum
7 likelihood estimates (MLEs) for the multistage model parameters (q_i) for each tumor type
8 are added together (*i. e.*, $\sum q_0, \sum q_1, \sum q_2$), and the resulting model is used to determine a
9 combined BMD. Then a confidence interval for the combined BMD is calculated by
10 computing the desired percentile of the chi-squared distribution associated with a likelihood
11 ratio test having one degree of freedom.

12
13 Once the organ-specific and multi-site BMDLs were obtained and scaled by body-weight,
14 the toxicokinetic model was used to estimate the continuous 24-hour air concentration that
15 would produce the same daily metabolized dose for an adult human (*i. e.*, the human
16 equivalent concentration or "HEC"). The cancer potency values were then calculated by
17 dividing the BMR of 0.05 by the HEC. Table 5 provides the calculated BMDs, BMDLs, and
18 the interspecies-adjusted BMDLs for individual and combined tumor sites. Potency values
19 derived from the primary studies are presented in Table 6 as unit risks factors (URFs) with
20 units of reciprocal $\mu\text{g}/\text{m}^3$.

21 Inhalation Potency Value for PCE

22
23 The updated carcinogenic potency value for PCE is based on the following observations
24 and rationale:

- 25
26 • Tissue-specific URF values calculated from the JISHA study are of similar
27 magnitude to the corresponding URFs obtained from the NTP study, though
28 somewhat lower. For mouse liver tumors, the ratio of the JISHA UR to the NTP UR
29 was about 0.8 in both females and males. For rat MCL the corresponding ratios
30 were 0.4 for females and 0.6 for males. The smaller URF values from the JISHA
31 data may be due in part to the higher precision obtained by the study having used
32 lower doses and an additional dose group.
- 33 • In both studies, the males of both species appeared to be more sensitive than the
34 corresponding females to the tumorigenic effects of PCE.
- 35 • The URF values from both studies ranged from 2.8E-06 to 1.6E-05 (per $\mu\text{g}/\text{m}^3$),
36 within a factor of 6. (The compared values included the multi-tumor risks for male
37 NTP rats and male JISHA mice, as well as tissue-specific risks for other organs in
38 mice and rats of both sexes.) Looking only at males of each species, the URFs
39 ranges from 4.0E-06 to 1.6E-05.
- 40 • The highest URF was obtained from the combined site (*i. e.*, multi-tumor) risk in
41 male rats in the NTP study. This value was obtained by including MCL, brain,
42 testicular, and renal tumors in the multi-tumor calculation.
- 43 • The URF values for mouse liver tumors and rat MCL were judged by OEHHA to be
44 more certain in view of the qualitative and quantitative agreement between the two
45 primary studies; mouse liver tumors were also found in the NCI (1977) oral
46 exposure study.

- 1 • The unique tumors seen in the NTP study, including kidney tumors, are important
2 to consider. The kidney is one site where the GST-pathway may contribute
3 substantially to the cancer potency. Moreover, there is reasonable evidence that
4 the GST-pathway may also contribute to tumorigenesis in other organ systems.
- 5 • Although it appears likely that PCE exposure increased the rate of testicular tumors
6 in rats, the relatively high risk value obtained for testicular tumors in NTP rats may
7 be more uncertain, given the high tumor incidence seen in the control group (71%).

8
9 Considering the above points, and also that the set of calculated values is clustered in a
10 narrow range, the geometric mean of the male mouse and rat URFs from both studies
11 was chosen as the best estimate of PCE cancer potency. Specifically, the geometric
12 mean was calculated using the URF values shown in Table 7. The resulting URF, when
13 rounded to two significant figures, is 6.1E-06 ($\mu\text{g}/\text{m}^3$)-1. A cancer slope factor of 2.1E-02
14 (per mg/kg-day) was also calculated from the URF using an adult body weight of 70 kg
15 and an inspiration rate of 20 m^3/day .
16

Table 5: BMD5 Modeling Results for the Primary Studies								
Study	Sex	Tumor Type	P-value for multi-stage model fit	Scaled residual for dose near the BMD	BMD (mg/kg-day)	BMDL (mg/kg-day)	Animal BW (kg)	BW-Scaled BMDL (mg/kg-day)
Results from Mouse Studies								
JISHA	M	Hepatocellular adenoma or carcinoma	0.22	1.17	3.06	2.16	0.048	0.350
		Harderian gland	0.99	-0.06	38.56	12.34	0.048	1.997
		Hemangioma or Hemangiosarcoma	0.35	0.94	26.61	12.98	0.048	2.100
		Combined site			2.73	1.85	0.048	0.300
	F	Hepatocellular adenoma or carcinoma	0.77	-0.23	10.33	3.84	0.035	0.574
NTP	M	Hepatocellular adenoma or carcinoma	0.85	0.03	2.46	1.79	0.037	0.272
	F	Hepatocellular adenoma or carcinoma	0.82	0.05	11.27	3.15	0.025	0.432
Results from Rat Studies								
JISHA	M	Mononuclear cell leukemia	0.79	0.07	1.34	0.89	0.45	0.251
	F	Mononuclear cell leukemia	0.37	1.05	3.99	1.84	0.30	0.472
NTP	M	Mononuclear cell leukemia	0.23	-0.31	0.92	0.51	0.44	0.144
		Testicular interstitial cell	0.35	-0.26	1.06	0.48	0.44	0.136
		Renal adenoma or carcinoma	0.93	0.07	6.76	3.24	0.44	0.913
		Brain glioma	0.15	0.62	9.45	5.07	0.44	1.426
		Combined site			0.46	0.28	0.44	0.078
	F	Mononuclear cell leukemia	0.25	-0.30	1.24	0.72	0.32	0.188

Table 6: Unit Risk Factors from Primary Studies					
Study	Sex	Tumor Type	BW-Scaled BMDL (mg/kg-day)	HEC based on PBPK Model (ppm)	Unit Risk Factor (URF) per $\mu\text{g}/\text{m}^3$
Results from Mouse Studies					
JISHA	M	Hepatocellular adenoma or carcinoma	0.350	2.14	3.5E-06
		Harderian gland	1.997	12.20	6.0E-07
		Hemangioma or Hemangiosarcoma	2.100	12.83	5.7E-07
		Combined site	0.300	1.83	4.0E-06
	F	Hepatocellular adenoma or carcinoma	0.574	3.51	2.1E-06
NTP	M	Hepatocellular adenoma or carcinoma	0.272	1.66	4.4E-06
	F	Hepatocellular adenoma or carcinoma	0.432	2.64	2.8E-06
Results from Rat Studies					
JISHA	M	Mononuclear cell leukemia	0.251	1.53	4.8E-06
	F	Mononuclear cell leukemia	0.472	2.88	2.6E-06
NTP	M	Mononuclear cell leukemia	0.144	0.88	8.4E-06
		Testicular interstitial cell	0.136	0.83	8.9E-06
		Renal adenoma or carcinoma	0.913	5.57	1.3E-06
		Brain glioma	1.426	8.71	8.5E-07
		Combined site	0.078	0.47	1.6E-05
	F	Mononuclear cell leukemia	0.188	1.15	6.4E-06

Table 7: URFs Used to Calculate Mean		
Species	Study	URF ($\mu\text{g}/\text{m}^3$)⁻¹
Male Mouse	JISHA (Multiple tumor)	4.02E-06
	NTP (Liver)	4.44E-06
Male Rat	JISHA (MCL)	4.81E-06
	NTP (Multiple tumor)	1.57E-05
	Geometric Mean	6.06E-06

1

1 **10. REFERENCES**

- 2 Anders MW, Lash L, Dekant W, Elfarra AA, Dohn DR, Reed DJ. 1988. Biosynthesis and
3 biotransformation of glutathioneS-conjugates to toxic metabolites. *CRC Critical Reviews in*
4 *Toxicology* 18:311-341.
- 5 Anderson EL. 1983. Quantitative Approaches in Use to Assess Cancer Risk. *Risk*
6 *Analysis* 3:277-295.
- 7 ARB. 2012. California Environmental Protection Agency, Air Resources Board, Air Toxic
8 Emissions Inventory, 2012.
- 9 Birner G, Richling C, Henschler D, Anders MW, Dekant W. 1994. Metabolism of
10 tetrachloroethene in rats: identification of N epsilon-(dichloroacetyl)-L-lysine and N
11 epsilon-(trichloroacetyl)-L-lysine as protein adducts. *Chemical Research in Toxicology*
12 7:724-732.
- 13 Birner G, Rutkowska A, Dekant W. 1996. N-acetyl-S-(1,2,2-trichlorovinyl)-L-cysteine and
14 2,2,2-trichloroethanol: Two novel metabolites of tetrachloroethene in humans after
15 occupational exposure. *Drug Metabolism and Disposition* 24:41-48.
- 16 Bull RJ, Sasser LB, Lei XC. 2004. Interactions in the tumor-promoting activity of carbon
17 tetrachloride, trichloroacetate, and dichloroacetate in the liver of male B6C3F₁ mice.
18 *Toxicology* 199:169-183.
- 19 CDHS. 1991. California Department of Health Services. Health Effects of
20 Tetrachloroethylene (PCE). Berkeley, CA.
- 21 Chiu WA, Ginsberg GL. 2011. Development and evaluation of a harmonized
22 physiologically based pharmacokinetic (PBPK) model for perchloroethylene toxicokinetics
23 in mice, rats, and humans. *Toxicology and Applied Pharmacology* 253:203-234.
- 24 Clewell HJ, Gentry PR, Kester JE, Andersen ME. 2005. Evaluation of physiologically
25 based pharmacokinetic models in risk assessment: an example with perchloroethylene.
26 *Critical Reviews in Toxicology* 35:413-433.
- 27 Dallas CE, Chen XM, O'Barr K, Muralidhara S, Varkonyi P, Bruckner JV. 1994.
28 Development of a physiologically based pharmacokinetic model for perchloroethylene
29 using tissue concentration-time data. *Toxicology and Applied Pharmacology* 128:50-59.
- 30 DeAngelo A B, Daniel FB, Wong DM, George MH. 2008. The induction of hepatocellular
31 neoplasia by trichloroacetic acid administered in the drinking water of the male B6C3F₁
32 mouse. *Journal of Toxicology and Environmental Health A71*:1056-1068.
- 33 Dekant W. 1986. Metabolic conversion of tri- and tetrachloroethylene: formation and
34 deactivation of genotoxic intermediates. *Developments in Toxicology & Environmental*
35 *Science* 12:211-221.
- 36 Dekant W, Birner G, Werner M, Parker J, 1998. Glutathione conjugation of
37 perchloroethene in subcellular fractions from rodent and human liver and kidney.
38 *Chemico-Biological Interactions* 116: 31-43.

- 1 Dekant W, Martens G, Vamvakas S, Metzler M, Henschler D. 1987. Bioactivation of
2 tetrachloroethylene: role of glutathione S-transferase-catalyzed conjugation versus
3 cCytochrome P-450-dependent phospholipid alkylation. *Drug Metabolism and Disposition*
4 15:702-709.
- 5 Dekant W, Metzler M, Henschler D. 1986. Identification of S-1,2,2-trichlorovinyl-N-
6 acetylcysteine as a urinary metabolite of tetrachloroethylene: bioactivation through
7 glutathione conjugation as a possible explanation of its nephrocarcinogenicity. *Journal of*
8 *Biochemical Toxicology* 1:57-72.
- 9 DeMarini DM, Perry E, Shelton ML. 1994. Dichloroacetic acid and related compounds:
10 induction of prophage in *E. coli* and mutagenicity and mutation spectra in *Salmonella*
11 TA100. *Mutagenesis* 9:429-437.
- 12 Dow. 2008. The Dow Chemical Company. Product Safety Assessment,
13 Perchloroethylene. June 24, 2008.
- 14 Emara AM, Abo El-Noor MM, Hassan NA, Wagih AA. 2010. Immunotoxicity and
15 hematotoxicity induced by tetrachloroethylene in Egyptian dry cleaning workers. *Inhalation*
16 *Toxicology* 22:117-124.
- 17 Fernandez J, Guberan E, Caperos J. 1976. Experimental human exposures to
18 tetrachloroethylene vapor and elimination in breath after inhalation. *American Industrial*
19 *Hygiene Association Journal* 37:143-150.
- 20 Frantz SW, Watanabe PG. 1983. Tetrachloroethylene: balance and tissue distribution in
21 male Sprague-Dawley rats by drinking-water administration. *Toxicology and Applied*
22 *Pharmacology* 69:66-72.
- 23 Green T, Odum J, Nash JA, Foster JR. 1990. Perchloroethylene-induced rat kidney
24 tumors: an investigation of the mechanisms involved and their relevance to humans.
25 *Toxicology and Applied Pharmacology* 103:77-89.
- 26 Guyton KZ, Chiu WA, Bateson TF, Jinot J, Scott CS, Brown RC, Caldwell JC. 2009. A
27 reexamination of the PPAR-alpha activation mode of action as a basis for assessing
28 human cancer risks of environmental contaminants. *Environmental Health Perspectives*
29 117:1664-1672.
- 30 Guyton KZ, Hogan KA, Scott CS, Cooper GS, Bale AS, Kopylev L, Barone S Jr, Makris
31 SL, Glenn B, Subramaniam RP, Gwinn MR, Dzubow RC, Chiu WA. 2014. Human health
32 effects of tetrachloroethylene: key findings and scientific issues. *Environmental Health*
33 *Perspectives* 122:325-334.
- 34 Hannon-Fletcher MP, Barnett YA. 2008. Lymphocyte cytochrome P450 expression:
35 inducibility studies in male Wistar rats. *British Journal of Biomedical Science* 65:1-6.
- 36 Hinchman CA, Ballatori N. 1994. Glutathione conjugation and conversion to mercapturic
37 acids can occur as an intrahepatic process. *Journal of Toxicology and Environmental*
38 *Health* 41:387-409.
- 39 HSDB. 2010. Hazardous Substance Data Bank. National Library of Medicine, Bethesda
40 MD. (Internet version accessed in 2015).

- 1 IARC. 1990. International Agency for Research on Cancer. Pathology of Tumors in
2 Laboratory Animals, 1: Tumours of the Rat. IARC Scientific Publication, No. 99, 2nd
3 edition, Lyon France.
- 4 IARC. 2014. International Agency for Research on Cancer. Trichloroethylene,
5 tetrachloroethylene, and some other chlorinated agents / IARC Working Group on the
6 Evaluation of Carcinogenic Risks to Humans (2012: Lyon, France). IARC monographs on
7 the evaluation of carcinogenic risks to humans. Vol 106.
- 8 Ikeda M, Koizumi A, Watanabe T, Endo A, Sato K. 1980. Cytogenetic and cytokinetic
9 investigations on lymphocytes from workers occupationally exposed to
10 tetrachloroethylene. *Toxicology Letters* 5: 251-256.
- 11 Irving RM, Elfarra AA. 2012. Role of reactive metabolites in the circulation in extrahepatic
12 toxicity. *Expert Opinion on Drug Metabolism & Toxicology* 8:1157-1172.
- 13 Irving RM, Elfarra AA. 2013. Mutagenicity of the cysteine S-conjugate sulfoxides of
14 trichloroethylene and tetrachloroethylene in the Ames test. *Toxicology* 306:157-161.
- 15 Ito Y, Yamanoshita O, Asaeda N, Tagawa Y, Lee CH, Aoyama T, Ichihara G, Furuhashi
16 K, Kamijima M, Gonzalez FJ, Nakajima T. 2007. Di(2-ethylhexyl)phthalate induces hepatic
17 tumorigenesis through a peroxisome proliferator-activated receptor alpha-independent
18 pathway. *Journal of Occupational Health* 49:172-182.
- 19 JISHA. 1993. Japan Industrial Safety and Health Association, Japan Bioassay Research
20 Center. Carcinogenicity study of tetrachloroethylene by inhalation in rats and mice. 2445
21 Hirasawa, Hadano, Kanagawa, 257-0015, Japan. March .31, 1993.
- 22 Kim S, Kim D, Pollack GM, Collins LB, Rusyn I. 2009. Pharmacokinetic analysis of
23 trichloroethylene metabolism in male B6C3F₁ mice: Formation and disposition of
24 trichloroacetic acid, dichloroacetic acid, S-(1,2-dichlorovinyl)glutathione and S-(1,2-
25 dichlorovinyl)-L-cysteine. *Toxicology and Applied Pharmacology* 238:90-9.
- 26 King-Herbert, Thayer. 2006. NTP workshop: Animal model for the NTP rodent cancer
27 bioassay: strain and stock - should we switch? *Toxicologic Pathology* 34: 802-805.
- 28 Klaunig JE, Babich MA, Baetcke KP, Cook JC, Corton JC, David RM, DeLuca JG, Lai DY,
29 McKee RH, Peters JM, Roberts RA, Fenner-Crisp PA. 2003. PPAR-alpha agonist-induced
30 rodent tumors: Modes of action and human relevance. *Critical Reviews in Toxicology*
31 33:655-780.
- 32 Kline SA, McCoy EC, Rosenkranz HS, Van Duuren BL. 1982. Mutagenicity of
33 chloroalkene epoxides in bacterial systems. *Mutation Research* 101:115-125.
- 34 Kroneld R. 1987. Effect of volatile halocarbons on lymphocytes and cells of the urinary
35 tract. *Bulletin of Environmental Contamination and Toxicology* 38:856-861.
- 36 Lash LH, Lipscomb JC, Putt DA, Parker JC. 1999. Glutathione conjugation of
37 trichloroethylene in human liver and kidney: kinetics and individual variation. *Drug*
38 *Metabolism and Disposition* 27:351-359.
- 39 Lash LH, Parker JC. 2001. Hepatic and renal toxicities associated with perchloroethylene.
40 *Pharmacological Reviews* 53:177-208.

- 1 Lash LH, Putt DA, Parker JC. 2006. Metabolism and Tissue Distribution of Orally
2 Administered Trichloroethylene in Male and Female Rats: Identification of Glutathione-
3 and Cytochrome P450-Derived Metabolites in Liver, Kidney, Blood and Urine. *Journal of*
4 *Toxicology and Environmental Health Part A* 69:1285-1309.
- 5 Lash LH, Putt DA, Huang P, Hueni SE, Parker JC. 2007. Modulation of hepatic and renal
6 metabolism and toxicity of trichloroethylene and perchloroethylene by alterations in status
7 of cytochrome P450 and glutathione. *Toxicology* 235:11-26.
- 8 Lash LH, Qian W, Putt DA, Desai K, Elfarra AA, Sicuri AR, Parker JC. 1998. Glutathione
9 conjugation of perchloroethylene in rats and mice in vitro: sex-, species-, and tissue-
10 dependent differences. *Toxicology and Applied Pharmacology*. 150:49-57.
- 11 Lehman-McKeeman, LD. 2010. 2u-Globulin Nephropathy, in McQueen, C. A.,
12 *Comprehensive toxicology*. 2nd ed. / Oxford: Elsevier, 2010.
- 13 Liao A, Broeg K, Fox T, Tan SF, Watters R, Shah MV, Zhang LQ, Li Y, Ryland L, Yang J,
14 Aliaga C, Dewey A, Rogers A, Loughran K, Hirsch L, Jarbada NR, Baab KT, Liao J,
15 Wang HG, Kester M, Desai D, Amin S, *et al.* 2011. Therapeutic efficacy of FTY720 in a rat
16 model of NK-cell leukemia. *Blood* 118:2793-2800.
- 17 Marth E. 1987. Metabolic changes following oral exposure to tetrachloroethylene in
18 subtoxic concentrations. *Archives of Toxicology* 60:293-299.
- 19 Mazzullo M, Grilli S, Lattanzi G, Prodi G, Turina MP, Colacci A. 1987. Evidence of DNA
20 binding activity of perchloroethylene. *Research Communications in Chemical Pathology &*
21 *Pharmacology* 58:215-235.
- 22 MDEP. 2014. Massachusetts Department of Environmental Protection, Office of
23 Research and Standards, Tetrachloroethylene (Perchloroethylene), Inhalation Unit Risk
24 Value, June 25, 2014.
- 25 NCI. 1977. National Cancer Institute. Bioassay of tetrachloroethylene for possible
26 carcinogenicity. Bethesda, Md: National Institutes of Health. Report no. NCI-CGTR-13;
27 DHEW Publication No. (NIH) 77-813.
- 28 NRC. 2010. National Research Council. Review of the Environmental Protection Agency's
29 draft IRIS assessment of tetrachloroethylene. National Academies Press, Washington
30 D.C.
- 31 NTP. 1986. National Toxicology Program, U.S. Department of Health and Human
32 Services. Toxicology and carcinogenesis studies of tetrachloroethylene
33 (perchloroethylene) (CAS no. 127-18-4) in F344/N rats and B6C3F1 mice (inhalation
34 studies). Research Triangle Park, NC. NTP Report no. TR 311.
- 35 NTP. 2014. National Toxicology Program, U.S. Department of Health and Human
36 Services. National Institutes of Health. 13th Report on Carcinogens. October 2, 2014.
- 37 Odum J, Green T, Foster JR, Hext PM. 1988. The role of trichloroacetic acid and
38 peroxisome proliferation in the differences in carcinogenicity of perchloroethylene in the
39 mouse and rat. *Toxicology and Applied Pharmacology* 92:103-112.

- 1 OEHHA. 1992. Office of Environmental Health Hazard Assessment. Health Effects of
2 Perchloroethylene. May 1992.
- 3 OEHHA. 2001. Office of Environmental Health Hazard Assessment. Public Health Goal
4 for Tetrachloroethylene in Drinking Water. August 2001.
- 5 OEHHA. 2009. Office of Environmental Health Hazard Assessment. Technical Support
6 Document for Cancer Potency Factors. May 2009.
- 7 OEHHA. 2012. Office of Environmental Health Hazard Assessment. Technical Support
8 Document for Exposure Assessment and Stochastic Analysis. August 2012.
- 9 Ohtsuki T, Sato K, Koizumi A, Kumai M, Ikeda M. 1983. Limited capacity of humans to
10 metabolize tetrachloroethylene. *International Archives of Occupational and Environmental*
11 *Health* 51:381-90.
- 12 Reddy MB. 2005. *Physiologically based pharmacokinetic modeling: science and*
13 *applications*. Wiley-Interscience.
- 14 Rooseboom M, Vermeulen NP, Groot EJ, Commandeur JN. 2002. Tissue distribution of
15 cytosolic beta-elimination reactions of selenocysteine Se-conjugates in rat and human.
16 *Chemico-Biological Interactions* 140:243-264.
- 17 Seiji K, Jin C, Watanabe T, Nakatsuka H, Ikeda M. 1990. Sister chromatid exchanges in
18 peripheral lymphocytes of workers exposed to benzene, trichloroethylene, or
19 tetrachloroethylene, with reference to smoking habits. *International Archives of*
20 *Occupational and Environmental Health* 62:171-176.
- 21 Schreiber JS, Hudnell HK, Geller AM, House DE, Aldous KM, Force MS, Langguth K,
22 Prohonic EJ, Parker JC, 2002. Apartment residents' and day care workers' exposures to
23 tetrachloroethylene and deficits in visual contrast sensitivity. *Environmental Health*
24 *Perspectives*. 110:655-664.
- 25 Sokol L, Loughran TP, Jr. 2006. Large granular lymphocyte leukemia. *Oncologist* 11:263-
26 273.
- 27 Thomas J, Haseman JK, Goodman JI, Ward JM, Loughran TP, Jr., Spencer PJ. 2007. A
28 review of large granular lymphocytic leukemia in Fischer 344 rats as an initial step toward
29 evaluating the implication of the endpoint to human cancer risk assessment. *Toxicological*
30 *Sciences* 99:3-19.
- 31 Tiruppathi C, Miyamoto Y, Ganapathy V, Roesel RA, Whitford GM, Leibach FH. 1990.
32 Hydrolysis and transport of proline-containing peptides in renal brush-border membrane
33 vesicles from dipeptidyl peptidase IV-positive and dipeptidyl peptidase IV-negative rat
34 strains. *Journal of Biological Chemistry* 265:1476-83.
- 35 Toraason M, Butler MA, Ruder A, Forrester C, Taylor L, Ashley DL, Mathias P, Marlow
36 KL, Cheever KL, Krieg E, Wey H. 2003. Effect of perchloroethylene, smoking, and race on
37 oxidative DNA damage in female dry cleaners. *Mutation Research/Genetic Toxicology*
38 *and Environmental Mutagenesis* 539:9-18.

- 1 Tucker JD, Sorensen KJ, Ruder AM, McKernan LT, Forrester CL, Butler MA. 2011.
2 Cytogenetic analysis of an exposed-referent study: perchloroethylene-exposed dry
3 cleaners compared to unexposed laundry workers. *Environmental Health* 10:16.
- 4 USEPA. 1991. Alpha-2u-globulin: Association with chemically induced renal toxicity and
5 neoplasia in the male rat. Washington, DC: U.S. Environmental Protection Agency,
6 National Center for Environmental Assessment. Report no. EPA/625/3-91/019F.
- 7 USEPA. 1992. Draft report: A cross-species scaling factor for carcinogen risk assessment
8 based on equivalence of mg/kg(3/4)/day. *Federal Register* 57:24151-24173.
- 9 USEPA. 2005. U.S. Environmental Protection Agency. Guidelines for carcinogen risk
10 assessment. Risk Assessment Forum. Report no. EPA/630/P-03/001F.
- 11 US EPA. 2011. U.S. Environmental Protection Agency. Toxicological Review of
12 Trichloroacetic Acid, In Support of Summary Information on the Integrated Risk
13 Information System (IRIS), Report no. EPA/635/R-09/003F.
- 14 US EPA. 2012a. U.S. Environmental Protection Agency. Toxicological Review of
15 Tetrachloroethylene (Perchloroethylene), In Support of Summary Information on the
16 Integrated Risk Information System (IRIS). Report no. EPA/635/R-08/011F.
- 17 US EPA. 2012b. U.S. Environmental Protection Agency. Integrated Risk Information
18 System (IRIS) Chemical Assessment Summary: Tetrachloroethylene (Perchloroethylene).
- 19 US EPA. 2012c. U.S. Environmental Protection Agency. Lymphohematopoietic Cancers
20 Induced by Chemicals and Other Agents: Overview and Implications for Risk Assessment,
21 EPA/600/R-10/095F.
- 22 US EPA. 2015. U.S. Environmental Protection Agency, National Center for Environmental
23 Assessment. Benchmark Dose Software (BMDS) Version 2.6.0.1.
- 24 Vamvakas S, Dekant W, Berthold K, Schmidt S, Wild D, Henschler D. 1987. Enzymatic
25 transformation of mercapturic acids derived from halogenated alkenes to reactive and
26 mutagenic intermediates. *Biochemical Pharmacology* 36:2741-2748.
- 27 Vamvakas S, Dekant W, Henschler D. 1989a. Genotoxicity of haloalkene and haloalkane
28 glutathione S-conjugates in porcine kidney cells. *Toxicology in Vitro* 3:151-156.
- 29 Vamvakas S, Herkenhoff M, Dekant W and Henschler D. 1989b. Mutagenicity of
30 tetrachloroethene in the Ames test—metabolic activation by conjugation with glutathione.
31 *Journal of Biochemical Toxicology*. 4:21–27.
- 32 Van Duuren BL, Kline SA, Melchionne S, Seidman I. 1983. Chemical structure and
33 carcinogenicity relationships of some chloroalkene oxides and their parent olefins. *Cancer*
34 *Research*. 43:159-162.
- 35 Vlaanderen J, Straif K, Ruder A, Blair A, Hansen J, Lynge E, Charbotel B, Loomis D,
36 Kauppinen T, Kyronen P, Pukkala E, Weiderpass E, Guha N. 2014. Tetrachloroethylene
37 exposure and bladder cancer risk: a meta-analysis of dry-cleaning-worker studies.
38 *Environmental Health Perspectives*. 122:661-666.

- 1 Volkel W, Friedewald M, Lederer E, Pahler A, Parker J, Dekant W, 1998.
- 2 Biotransformation of perchloroethene: dose-dependent excretion of trichloroacetic acid,
- 3 dichloroacetic acid, and N-acetyl-S-(trichlorovinyl)-L-cysteine in rats and humans after
- 4 inhalation. *Toxicology and Applied Pharmacology*. 153:20-27.
- 5 Walles SA. 1986. Induction of single-strand breaks in DNA of mice by trichloroethylene
- 6 and tetrachloroethylene. *Toxicology Letters* 31:31-35.
- 7 Wang JL, Chen WL, Tsai SY, Sung PY, Huang RN. 2001. An *in vitro* model for evaluation
- 8 of vaporous toxicity of trichloroethylene and tetrachloroethylene to CHO-K1 cells.
- 9 *Chemico-Biological Interactions* 137:139-154.
- 10 Wheeler JB, Stourman NV, Their R, Dommermuth A, Vuilleumier S, Rose JA, Armstrong
- 11 RN, Guengerich FP, 2001. Conjugation of haloalkanes by bacterial and mammalian
- 12 glutathione transferases: mono- and dihalomethanes. *Chemical Research in Toxicology*
- 13 14:1118-1127.
- 14 White IN, Razvi N, Gibbs AH, Davies AM, Manno M, Zaccaro C, De Matteis F, Pahler A,
- 15 Dekant W. 2001. Neoantigen formation and clastogenic action of HCFC-123 and
- 16 perchloroethylene in human MCL-5 cells. *Toxicology Letters* 124:129-138.
- 17 Yang Q, Ito S, Gonzalez FJ. 2007. Hepatocyte-restricted constitutive activation of PPAR
- 18 alpha induces hepatoproliferation but not hepatocarcinogenesis. *Carcinogenesis* 28:1171-
- 19 1177.
- 20 Yoo HS, Bradford BU, Kosyk O, Shymonyak S, Uehara T, Collins LB, Bodnar WM, Ball
- 21 LM, Gold A, Rusyn I. 2015. Comparative analysis of the relationship between
- 22 trichloroethylene metabolism and tissue-specific toxicity among inbred mouse strains: liver
- 23 effects. *Journal of Toxicology and Environmental Health A*. 78:15-31.
- 24 Yoshioka T, Krauser JA, Guengerich FP. 2002. Tetrachloroethylene oxide: hydrolytic
- 25 products and reactions with phosphate and lysine. *Chemical Research in Toxicology*
- 26 15:1096-1105.
- 27

1
2
3
4
5
6
7
8
9
10
11
12
13
14
15
16
17
18
19
20

APPENDIX A

**PBPK Model Code for Simplified, Inhalation-Only Adaptation of Chiu and Ginsberg
(2011) PCE Model, for Mice, Rats, and Humans
(Written in Berkeley Madonna)**

{ Inhalation-Only Adaptation of Chiu and Ginsberg (2010) PCE Model
for MICE }

```
1
2
3
4 METHOD RK4
5 STARTTIME = 0
6 STOPTIME=504
7 DT = 0.002
8
9 ppm=10      {inhaled conc in ppm}
10 CInh=If (Mod(Time,24)<=6 AND Mod(Time,168)<=120) Then (ppm*165.83/24450) Else 0
11
12 ; BW=0.037 {NTP Male}
13 ; BW=0.048 {JISHA Male}
14 ; BW=0.025 {NTP Female}
15   BW=0.035 {JISHA Female}
16
17 QC=11.6*BW^0.75
18 QP=QC*2.5*exp(0.325015)
19 QM=QP/0.7   {minute volume, L/h}
20 DResp=QP*exp(0.203)
21 ; Intake=QM*Cinh*24/BW
22
23 QGut=0.141*QC
24 QLiv=0.02*QC
25 QKid=0.091*QC
26 QFat=0.07*QC
27 QRap=0.461*QC
28 QSlw=0.217*QC
29
30 PB=18.6
31 PResp=79.1/PB
32 PGut=62.1/PB
33 PLiv=48.8/PB
34 PKid=79.1/PB
35 PRap=62.1/PB
36 PSlw=79.1/PB
37 PFat=1510.8/PB
38
39 VResp=0.0007*BW
40 VRespEff=VResp*PResp*PB
41 VRespLum=0.004667*BW
42 VGut=0.049*BW
43 VLiv=0.055*BW
44 VKid=0.017*BW
45 VRap=0.1*BW
46 VFat=0.07*BW
47 VBld=0.049*BW
48 VSlw=(0.8897*BW)-(VResp+VGut+VLiv+VKid+VRap+VFat+VBld)
49
50 { Metabolic Constant Calculations }
51 {=====}
52 KMo=          88.6
53 lnKMC=        -5.35885
54 ClCo=         1.57
55 lnClC=        3.18103
56 lnKM2C=       15
57 lnCl2OxC=     -1.20051
58 KmKidLivo=    0.616
```

Perchloroethylene Inhalation Cancer Potency Values
SRP REVIEW DRAFT

May, 2016 (revised)

```

1  ClKidLivo=          0.0211
2  VMaxLungLivo=      0.07
3  VMaxTCVGo=         35.3
4  lnVMaxTCVGC=       10.2
5  ClTCVGo=           0.656
6  lnClTCVGC=         -9.17006
7  VMaxKidLivTCVGo=   0.15
8  ClKidLivTCVGo=     0.24
9
10 KM=KMo*exp(lnKMC)
11 VMax= KM*ClCo*VLiv*exp(lnClC)
12
13 KM2=KM*exp(lnKM2C)
14 VMax2=KM2*(VMax/KM)*exp(lnCl2OxC)
15
16 KMKid=KM*KMKidLivo
17 VMaxKid=(VMax/KM)*KMKid*(VKid/VLiv)*ClKidLivo
18
19 KMClara=KM*PLiv/(PB*PResp)
20 VMaxClara=VMax*VMaxLungLivo
21
22 VMaxTCVG=VMaxTCVGo*VLiv*exp(lnVMaxTCVGC)
23 KmTCVG=VMaxTCVG/(ClTCVGo*exp(lnClTCVGC))
24
25 VMaxKidTCVG=VMaxTCVG*(VKid/VLiv)*VMaxKidLivTCVGo
26 KmKidTCVG=VMaxKidTCVG/(ClKidLivTCVGo*(VKid/VLiv)*(VMaxTCVG/KMTCVG))
27 {=====}
28
29 Init AGut=0          Limit AGut>=0
30 Init AResp=0         Limit AResp>=0
31 Init AExhResp=0      Limit AExhResp>=0
32 Init AInhResp=0      Limit AInhResp>=0
33 Init ALiv=0           Limit ALiv>=0
34 Init AKid=0           Limit AKid>=0
35 Init ARap=0           Limit ARap>=0
36 Init ASlw=0           Limit ASlw>=0
37 Init AFat=0           Limit AFat>=0
38 Init ABld=0           Limit ABld>=0
39
40 {Respiratory Model Concentrations}
41 CInhResp=AInhResp/VRespLum      {conc resp lumen during inh, mg/L}
42 CResp=AResp/VRespEff            {conc resp tract tissue, mg/L}
43 CExhResp=AExhResp/VRespLum     {conc resp lumen during exh, mg/L}
44
45 {Blood Concentrations}
46 CVGut=(AGut/VGut)*(1/PGut)
47 CVLiv=(ALiv/VLiv)*(1/PLiv)
48 CVKid=(AKid/VKid)*(1/PKid)
49 CVRap=(ARap/VRap)*(1/PRap)
50 CVSlw=(ASlw/VSlw)*(1/PSlw)
51 CVFat=(AFat/VFat)*(1/PFat)
52 CVBld=(ABld/VBld)
53 CArt=(QC*CVBld+QP*CInhResp)/(QC+(QP/PB))
54
55 {Metabolism: P450 Oxidation}
56 RAMetLng=(VMaxClara*CResp)/(KMClara+CResp)
57 RAMetLiv1=(VMax*CVLiv)/(KM+CVLiv)+(VMax2/KM2)*CVLiv
58 RAMetKid1=(VMaxKid*CVKid)/(KMKid+CVKid)
59

```

```
1 {Metabolism: GST Conjugation}
2 RAMetLiv2=(VMaxTCVG*CVLiv)/(KMTCVG+CVLiv)
3 RAMetKid2=(VMaxKidTCVG*CVKid)/(KMKidTCVG+CVKid)
4
5 {Respiratory Model Mass Balance Equations}
6 AInhResp'=QM*CIInh+DResp*(CResp-CInhResp)-QM*CIInhResp
7 AResp'=DResp*(CInhResp+CEXHResp-2*CResp)-RAMetLNg
8 AExhResp'=QM*(CInhResp-CEXHResp)+QP*((CArt/PB)-CInhResp)+DResp*(CResp-CEXHResp)
9
10 {Other Mass Balance Equations}
11 AGut'=QGut*(CArt-CVGut)
12 ALiv'=(QLiv*CArt)+(QGut*CVgut)-((QLiv+QGut)*CVLiv)-RAMetLiv1-RAMetLiv2
13 AKid'=QKid*(CArt-CVKid)-RAMetKid1-RAMetKid2
14 ARap'=Qrap*(CArt-CVRap)
15 ASlw'=QSlw*(CArt-CVSlw)
16 AFat'=QFat*(CArt-CVfat)
17 ABld'=(QFat*CVfat)+((QGut+QLiv)*CVLiv)+(QSlw*CVSlw)+(Qrap*CVRap)+(QKid*CVKid)-
18 (QC*CVBld)
19
20 init MetCum=0          Limit MetCum>=0
21 init LivOxCum=0       Limit LivOxCum>=0
22
23 MetTot=RAMetLNg+RAMetLiv1+RAMetKid1+RAMetLiv2+RAMetKid2
24 MetCum'=If TIME>=336 Then (MetTot/(7*BW)) Else 0
25 LivOxCum'=If TIME>=336 Then (RAMetLiv1/(7*BW)) Else 0
26
```

{ Inhalation-Only Adaptation of Chiu and Ginsberg (2011) PCE Model
for RATS }

```
1
2
3
4 METHOD RK4
5 STARTTIME = 0
6 STOPTIME=504
7 DT = 0.002
8
9 ppm=50      {inhaled conc in ppm}
10 CInh=If (Mod(Time,24)<=6 AND Mod(Time,168)<=120) Then (ppm*165.83/24450) Else 0
11
12 ; BW=0.44   {NTP Male}
13   BW=0.45   {JISHA Male}
14 ; BW=0.32   {NTP Female}
15   BW=0.30   {JISHA Female}
16
17 QC=13.3*BW^0.75
18 QP=QC*1.9*0.61643
19 QM=QP/0.7   {minute volume, L/h}
20 DResp=QP*exp(1)
21 ; Intake=QM*CInh*24/BW
22
23 QGut=0.153*QC
24 QLiv=0.021*QC
25 QKid=0.141*QC
26 QFat=0.07*QC
27 QRap=0.279*QC
28 QSlw=0.336*QC
29
30 PB=15.1
31 PResp=32.7/PB
32 PGut=40.6/PB
33 PLiv=50.3/PB
34 PKid=32.7/PB
35 PRap=40.4/PB
36 PSlw=21.6/PB
37 PFat=1489.3/PB
38
39 VResp=0.0005*BW
40 VRespEff=VResp*PResp*PB
41 VRespLum=0.004667*BW
42 VGut=0.032*BW
43 VLiv=0.034*BW
44 VKid=0.007*BW
45 VRap=0.088*BW
46 VFat=0.07*BW
47 VBld=0.074*BW
48 VSlw=(0.8995*BW)-(VResp+VGut+VLiv+VKid+VRap+VFat+VBld)
49
50 { Metabolic Constant Calculations }
51 {=====}
52 KMo=          69.7
53 lnKMC=        -0.805889
54 ClCo=          0.36
55 lnClC=        2.02965
56 KMKidLivo=    1.53
57 ClKidLivo=    0.0085
58 VMaxLungLivo= 0.0144
```

Perchloroethylene Inhalation Cancer Potency Values
SRP REVIEW DRAFT

May, 2016 (revised)

```

1  VmaxTCVGo=          93.9
2  lnVMaxTCVGC=       10.2
3  ClTCVGo=           2.218
4  lnClTCVGC=        -6.99311
5  VMaxKidLivTCVGo=   0.15
6  ClKidLivTCVGo=     0.098
7
8  KM=KMo*exp(lnKMC)
9  VMax=KM*ClCo*VLiv*exp(lnClC)
10
11 KMKid=KM*KMKidLivo
12 VMaxKid=(VMax/KM)*KMKid*(VKid/VLiv)*ClKidLivo
13
14 KMClara=KM*PLiv/(PB*PResp)
15 VMaxClara=VMax*VMaxLungLivo
16
17 VMaxTCVG=VMaxTCVGo*VLiv*exp(lnVMaxTCVGC)
18 KmTCVG=VMaxTCVG/(ClTCVGo*exp(lnClTCVGC))
19
20 VMaxKidTCVG=VMaxTCVG*(VKid/VLiv)*VMaxKidLivTCVGo
21 KmKidTCVG=VMaxKidTCVG/(ClKidLivTCVGo*(VKid/VLiv)*(VMaxTCVG/KMTCVG))
22 {=====}
23
24 Init AGut=0          Limit AGut>=0
25 Init AResp=0         Limit AResp>=0
26 Init AExhResp=0     Limit AExhResp>=0
27 Init AInhResp=0     Limit AInhResp>=0
28 Init ALiv=0          Limit ALiv>=0
29 Init AKid=0           Limit AKid>=0
30 Init ARap=0           Limit ARap>=0
31 Init ASlw=0           Limit ASlw>=0
32 Init AFat=0           Limit AFat>=0
33 Init ABld=0           Limit ABld>=0
34
35 {Respiratory Model Concentrations}
36 CInhResp=AInhResp/VRespLum {conc resp lumen during inh, mg/L}
37 CResp=AResp/VRespEff      {conc resp tract tissue, mg/L}
38 CExhResp=AExhResp/VRespLum {conc resp lumen during exh, mg/L}
39
40
41 {Blood Concentrations}
42 CVGut=(AGut/VGut)*(1/PGut)
43 CVLiv=(ALiv/VLiv)*(1/PLiv)
44 CVKid=(AKid/VKid)*(1/PKid)
45 CVRap=(ARap/VRap)*(1/PRap)
46 CVSlw=(ASlw/VSlw)*(1/PSlw)
47 CVFat=(AFat/VFat)*(1/PFat)
48 CVBld=(ABld/VBld)
49 CArt=(QC*CVBld+QP*CInhResp)/(QC+(QP/PB))
50
51 {Metabolism: P450 Oxidation}
52 RAMetLiv1=(VMax*CVLiv)/(KM+CVLiv)
53 RAMetKid1=(VMaxKid*CVKid)/(KMKid+CVKid)
54 RAMetLng=(VMaxClara*CResp)/(KMClara+CResp)
55
56 {Metabolism: GST Conjugation}
57 RAMetLiv2=(VMaxTCVG*CVLiv)/(KMTCVG+CVLiv)
58 RAMetKid2=(VMaxKidTCVG*CVKid)/(KMKidTCVG+CVKid)
59

```

```
1 {Respiratory Model Mass Balance Equations}
2 AInhResp'=QM*CIInh+DResp*(CResp-CInhResp)-QM*CIInhResp
3 AResp'=DResp*(CInhResp+CEXhResp-2*CResp)-RAMetLng
4 AExhResp'=QM*(CInhResp-CEXhResp)+QP*((CART/PB)-CInhResp)+DResp*(CResp-CEXhResp)
5
6 {Other Mass Balance Equations}
7 AGut'=QGut*(CART-CVGut)
8 ALiv'=(QLiv*CART)+(QGut*CVgut)-((QLiv+QGut)*CVLiv)-RAMetLiv1-RAMetLiv2
9 AKid'=QKid*(CART-CVKid)-RAMetKid1-RAMetKid2
10 ARap'=Qrap*(CART-CVRap)
11 ASlw'=QSlw*(CART-CVSlw)
12 AFat'=QFat*(CART-CVFat)
13 ABld'=(QFat*CVFat)+((QGut+QLiv)*CVLiv)+(QSlw*CVSlw)+(Qrap*CVRap)+(QKid*CVKid)-
14 (QC*CVBld)
15
16 init MetCum=0      Limit MetCum>=0
17
18 MetTot=RAMetLng+RAMetLiv1+RAMetKid1+RAMetLiv2+RAMetKid2
19 MetCum'=If TIME>=336 Then (MetTot/(7*BW)) Else 0
20
```

{ Inhalation-Only Adaptation of Chiu and Ginsberg (2011) PCE Model
for HUMANS }

```
1
2
3
4 METHOD RK4
5 STARTTIME=0
6 STOPTIME=840
7 DT = 0.0002
8
9 ppm=10      {inhaled conc in ppm}
10 CInh=ppm*165.83/24450
11
12 BW=70
13 QC=16*BW^0.75
14 QP=0.96*1.28*QC
15 QM=QP/0.7  {minute volume, L/h}
16 DResp=QP*exp(-5.06)
17 ; Intake=QM*Cinh
18
19 QGut=0.19*QC
20 QLiv=0.065*QC
21 QKid=0.19*QC
22 QFat=0.05*QC
23 QRap=0.285*QC
24 QSlw=0.22*QC
25
26 PB=14.7
27 PResp=58.6/PB
28 PGut=59.9/PB
29 PLiv=61.1/PB
30 PKid=58.6/PB
31 PRap=59.9/PB
32 PSlw=70.5/PB
33 PFat=1450/PB
34
35 VResp=0.00018*BW
36 VRespEff=VResp*PResp*PB
37 VRespLum=0.002386*BW
38 VGut=0.02*BW
39 VLiv=0.025*BW
40 VKid=0.0043*BW
41 VRap=0.088*BW
42 VFat=0.199*BW
43 VBld=0.077*BW
44 VSlw=(0.8560*BW)-(VResp+VGut+VLiv+VKid+VRap+VFat+VBld)
45
46 { Metabolic Constant Calculations }
47 {=====}
48 KMo=          55.8
49 lnKMC=        6.9
50 ClCo=         0.202
51 lnClC=        0.2501
52 KMKidLivo=    1.04
53 ClKidLivo=    0.0125
54 lnClKidLivC=  4.57452
55 VMaxLungLivo= 0.0128
56 VMaxTCVGo=    0.665
57 lnVMaxTCVGC= 10.2
58 ClTCVGo=      0.0196
```

Perchloroethylene Inhalation Cancer Potency Values
SRP REVIEW DRAFT

May, 2016 (revised)

```

1  lnClTCVGC=          5.59162
2  VMaxKidLivTCVGo=    0.15
3  ClKidLivTCVGo=      0.14
4
5  KM=KMo*exp(lnKMC)
6  VMax=KM*ClCo*VLiv*exp(lnClC)
7
8  KMKid=KM*KMKidLivo
9  VMaxKid=(VMax/KM)*KMKid*(VKid/VLiv)*ClKidLivo*exp(lnClKidLivC)
10
11 KMClara=KM*PLiv/(PB*PResp)
12 VMaxClara=VMax*VMaxLungLivo
13
14 VMaxTCVG=VMaxTCVGo*VLiv*exp(lnVMaxTCVGC)
15 KmTCVG=VMaxTCVG/(ClTCVGo*exp(lnClTCVGC))
16
17 VMaxKidTCVG=VMaxTCVG*(VKid/VLiv)*VMaxKidLivTCVGo
18 KmKidTCVG=VMaxKidTCVG/(ClKidLivTCVGo*(VKid/VLiv)*(VMaxTCVG/KMTCVG))
19 {=====}
20
21 {Metabolism: P450 Oxidation}
22 RAMetLiv1=(Vmax*CVLiv)/(KM+CVLiv)
23 RAMetKid1=(VMaxKid*CVKid)/(KMKid+CVKid)
24 RAMetLng=(VMaxClara*CResp)/(KMClara+CResp)
25
26 {Metabolism: GST Conjugation}
27 RAMetLiv2=(VMaxTCVG*CVLiv)/(KMTCVG+CVLiv)
28 RAMetKid2=(VMaxKidTCVG*CVKid)/(KMKidTCVG+CVKid)
29
30 Init AGut=0          Limit AGut>=0
31 Init AResp=0         Limit AResp>=0
32 Init AExhResp=0     Limit AExhResp>=0
33 Init AInhResp=0     Limit AInhResp>=0
34 Init ALiv=0          Limit ALiv>=0
35 Init AKid=0          Limit AKid>=0
36 Init ARap=0          Limit ARap>=0
37 Init ASlw=0          Limit ASlw>=0
38 Init AFat=0          Limit AFat>=0
39 Init ABld=0          Limit ABld>=0
40
41 {Respiratory Model Concentrations}
42 CInhResp=AInhResp/VRespLum {conc resp lumen during inh, mg/L}
43 CResp=AResp/VRespEff      {conc resp tract tissue, mg/L}
44 CExhResp=AExhResp/VRespLum {conc resp lumen during exh, mg/L}
45
46 {Blood Concentrations}
47 CVGut=(AGut/VGut)*(1/PGut)
48 CVLiv=(ALiv/VLiv)*(1/PLiv)
49 CVKid=(AKid/VKid)*(1/PKid)
50 CVRap=(ARap/VRap)*(1/PRap)
51 CVSlw=(ASlw/VSlw)*(1/PSlw)
52 CVFat=(AFat/VFat)*(1/PFat)
53 CVBld=(ABld/VBld)
54 CArt=(QC*CVBld+QP*CInhResp)/(QC+(QP/PB)) {arterial blood conc}
55
56 {Respiratory Model Mass Balance Equations}
57 AInhResp'=QM*CInh+DResp*(CResp-CInhResp)-QM*CInhResp
58 AResp'=DResp*(CInhResp+CExhResp-2*CResp)-RAMetLng
59 AExhResp'=QM*(CInhResp-CExhResp)+QP*((CArt/PB)-

```

1 $C_{InhResp} + D_{Resp} * (C_{Resp} - C_{ExhResp})$
2
3 {Other Mass Balance Equations}
4 $A_{Gut} = Q_{Gut} * (C_{Art} - C_{VGut})$
5 $A_{Liv} = (Q_{Liv} * C_{Art}) + (Q_{Gut} * C_{Vgut}) - ((Q_{Liv} + Q_{Gut}) * C_{VLiv}) - RAMetLiv1 - RAMetLiv2$
6 $A_{Kid} = Q_{Kid} * (C_{Art} - C_{VKid}) - RAMetKid1 - RAMetKid2$
7 $A_{Rap} = Q_{rap} * (C_{Art} - C_{VRap})$
8 $A_{Slw} = Q_{Slw} * (C_{Art} - C_{VSlw})$
9 $A_{Fat} = Q_{Fat} * (C_{Art} - C_{VFat})$
10 $A_{Bld} = (Q_{Fat} * C_{VFat}) + ((Q_{Gut} + Q_{Liv}) * C_{VLiv}) + (Q_{Slw} * C_{VSlw}) + (Q_{Rap} * C_{VRap}) + (Q_{Kid} * C_{VKid}) -$
11 $(Q_C * C_{VBld})$
12
13 $MetTot = (RAMetLng + RAMetLiv1 + RAMetKid1 + RAMetLiv2 + RAMetKid2) * (24 / BW)$
14

1
2
3
4
5
6
7
8
9
10
11
12
13
14
15
16
17
18

APPENDIX B

**Dose Metric Values used in Dose-Response Modeling
Obtained from PBPK Inhalation Model**

1

PBPK Estimated Total Metabolized Doses
(mg/kg-day)

JISHA Mouse (Male and female weights: 0.048 and 0.035 kg)		
Exposure Concentration (ppm)	Male	Female
10	5.10	5.22
50	18.15	18.44
250	72.73	73.94
JISHA Rat (Male and female weights: 0.45 and 0.30 kg)		
Exposure Concentration (ppm)	Male	Female
50	1.82	1.88
200	6.47	6.67
600	15.32	15.83
NTP Mouse (Male and female weights: 0.037 and 0.025 kg)		
Exposure Concentration (ppm)	Male	Female
100	32.78	33.38
200	60.25	61.40
NTP Rat (Male and female weights: 0.44 and 0.32 kg,		
Exposure Concentration (ppm)	Male	Female
200	6.48	6.63
400	11.38	11.66

2

3